

## Many pion decays of $\rho(770)$ and $\omega(782)$ mesons in chiral theory.

N. N. Achasov \* and A. A. Kozhevnikov †

*Laboratory of Theoretical Physics,  
Sobolev Institute for Mathematics  
630090, Novosibirsk-90, Russia*

(October 25, 2018)

### Abstract

The decays  $\rho(770) \rightarrow 4\pi$  and  $\omega(782) \rightarrow 5\pi$  are considered in detail in the approach based on the Weinberg Lagrangian obtained upon the nonlinear realization of chiral symmetry, added with the term induced by the anomalous Lagrangian of Wess and Zumino. The partial widths and excitation curves of the decays  $\rho^0 \rightarrow 2\pi^+2\pi^-$ ,  $\pi^+\pi^-2\pi^0$ ,  $\rho^\pm \rightarrow 2\pi^\pm\pi^\mp\pi^0$ ,  $\rho^\pm \rightarrow \pi^\pm 3\pi^0$  are evaluated for  $e^+e^-$  annihilation, photoproduction and  $\tau$  lepton decays. The results of calculations are compared with the recent CMD-2 data on the decay  $\rho^0 \rightarrow 2\pi^+2\pi^-$  observed in  $e^+e^-$  annihilation. The  $\omega \rightarrow 5\pi$  decay widths and excitation curves in  $e^+e^-$  annihilation are obtained. The angular distributions for various combinations of the final pions in the decays  $\rho \rightarrow 4\pi$  and  $\omega \rightarrow 5\pi$  are written. The perspectives of the experimental study of the above decays in  $e^+e^-$  annihilation,  $\tau$  lepton decays and photoproduction are discussed.

11.30.Rd;12.39.Fe;13.30 Eg

Typeset using REVTeX

---

\*Electronic address: achasov@math.nsc.ru

†Electronic address: kozhev@math.nsc.ru

## I. INTRODUCTION

Despite the lack of a straightforward derivation from first principles of QCD, the effective Lagrangians that describe the low-energy interactions of the ground state octet of pseudoscalar mesons  $\pi$ ,  $K$ ,  $\eta$  are constructed upon treating these mesons as the Goldstone bosons of the spontaneously broken chiral  $U_L(3) \times U_R(3)$  symmetry of the massless three-flavored QCD Lagrangian. The key point in this task is that the transformation properties of the Goldstone fields under the nonlinear realization of chiral symmetry are sufficient for the establishing the most general form of the effective Lagrangian [1]. As far as vector mesons are concerned, the situation is not so clear, because the vector mesons, contrary to the pseudoscalar ones, cannot be considered as the Goldstone bosons of the spontaneously broken symmetry. For this reason there exist different schemes of including these mesons into the effective chiral Lagrangians. The scheme of Ref. [2] where the vector mesons are treated as the dynamical gauge bosons of hidden local symmetry (HLS), incorporates these mesons into the effective chiral Lagrangian in a most elegant way. However, a straightforward comparison with the data of the predictions of these models immediately meets with difficulty, since the dominant decay modes of all the ground state vector mesons produce pseudoscalar mesons that are far from being soft. This means that both the higher derivatives in the low energy expansion of the effective Lagrangians and the loop quantum corrections should be taken into account.

We suggest here many pion decay modes of  $\rho(770)$  and  $\omega(782)$  mesons as a test ground for the chiral models of vector mesons [3,4]. Theoretically, pions in the final state in such decays are soft to the extent to be specified below. This fact allows one to neglect the higher derivative and loop corrections in the effective Lagrangian. On the other hand, the unconventional, from the point of view of the chiral pion dynamics, sources of soft pions are feasible. Indeed, the progress in increasing the intensity of low energy  $e^+e^-$  colliders ( $\phi$  factories) [5], photon beams [6], and a huge number of the specific hadronic decays of  $\tau$  leptons could offer the naturally controlled sources of soft pions, provided the sufficiently low invariant mass regions of hadronic systems are isolated. The yield of pions is considerably enhanced when they are produced through the proper vector resonance states, which will hopefully offer the possibility of testing the mentioned models.

Pions emitted in the decay  $\rho \rightarrow 4\pi$  are rather soft, because their typical momentum is  $|\mathbf{p}| \sim m_\pi$ , where  $m_\pi$  is the pion mass. By this reason this decay attracts much attention [7–10] from the point of view of the study of the predictions of the effective chiral Lagrangians for vector mesons. As was found in Refs. [7–9], the above decay should be rather strong,  $B(\rho \rightarrow 4\pi) \sim 10^{-4}$ . The calculations of Refs. [8,9] were analyzed in detail in Ref. [10], where a number of shortcomings of the former related with the actual violation of chiral invariance, in particular, the Adler condition [11] for soft pions, was uncovered. The correct results based on the amplitudes obeying the Adler condition and obtained in Refs. [3,10], correspond to  $B(\rho \rightarrow 4\pi) \approx 10^{-5}$ . The large magnitude of the branching ratio  $B(\rho \rightarrow 4\pi) \sim 10^{-4}$  obtained in Ref. [7] is related, in all appearance, with a very rough method of calculation. A common drawback of Refs. [7–10] is that their authors evaluate the partial width at the only energy equal to the mass of the  $\rho$ , as if the latter were a genuine narrow peak. However, the fact that the width of the  $\rho$  resonance is rather large, and  $\Gamma(\rho \rightarrow 4\pi, E)$  rises rapidly with the energy increase even at energies inside the  $\rho$  peak, forces one to think that the magnitude

of the  $4\pi$  partial width at the  $\rho$  mass cannot be an adequate characteristics of the dynamics of the process. In this respect, it is just the resonance excitation curve in the channel  $e^+e^- \rightarrow \rho^0 \rightarrow 4\pi$  which is of much interest, being a test ground of various chiral models of the decay under consideration.

Pions emitted in the decay  $\omega \rightarrow 5\pi$  [4] are truly soft, because they possess the typical momentum  $|\mathbf{p}| \simeq 0.5m_\pi$ . Hence, the lowest order terms obtained upon neglecting the higher derivatives and loop corrections should give the reliable results.

The aim of the present paper is to consider in detail the many pion decay modes of the vector  $\rho(770)$  and  $\omega(782)$  mesons in the framework of the effective chiral Lagrangian approach. The first Lagrangian of this kind incorporating the isotopic triplets of the  $\rho$  meson field  $\boldsymbol{\rho}_\mu$ , the pion field  $\boldsymbol{\pi}$ , and their interaction was proposed by Weinberg [12] under the nonlinear realization of the chiral symmetry

$$\begin{aligned} \mathcal{L}^{(\rho+\pi)} = & -\frac{1}{4} (\partial_\mu \boldsymbol{\rho}_\nu - \partial_\nu \boldsymbol{\rho}_\mu + g[\boldsymbol{\rho}_\mu \times \boldsymbol{\rho}_\nu])^2 \\ & + \frac{m_\rho^2}{2} \left[ \boldsymbol{\rho}_\mu + \frac{[\boldsymbol{\pi} \times \partial_\mu \boldsymbol{\pi}]}{2gf_\pi^2(1 + \boldsymbol{\pi}^2/4f_\pi^2)} \right]^2 \\ & + \frac{(\partial_\mu \boldsymbol{\pi})^2}{2(1 + \boldsymbol{\pi}^2/4f_\pi^2)^2} - \frac{m_\pi^2 \boldsymbol{\pi}^2}{2(1 + \boldsymbol{\pi}^2/4f_\pi^2)}, \end{aligned} \quad (1.1)$$

where  $f_\pi = 92.4$  MeV is the pion decay constant, and the cross denotes the vector product in the isovector space. As was shown, the Lagrangian Eq. (1.1) results from the HLS approach [2]. The  $\rho\rho\rho$  coupling constant  $g$  and the  $\rho\pi\pi$  coupling constant  $g_{\rho\pi\pi}$  are related to the  $\rho$  mass  $m_\rho$  and the pion decay constant  $f_\pi$  via the parameter of hidden local symmetry  $a$  as [2]

$$\begin{aligned} g &= m_\rho/f_\pi\sqrt{a}, \\ g_{\rho\pi\pi} &= \sqrt{a}m_\rho/2f_\pi. \end{aligned} \quad (1.2)$$

Note that  $a = 2$ , if one demands the universality condition  $g = g_{\rho\pi\pi}$  to be satisfied. Then the so called Kawarabayashi-Suzuki-Riazuddin-Fayyazuddin (KSRF) relation [13] arises

$$2g_{\rho\pi\pi}^2 f_\pi^2 / m_\rho^2 = 1 \quad (1.3)$$

which beautifully agrees with experiment. The  $\rho\pi\pi$  coupling constant resulting from this relation is  $g_{\rho\pi\pi} = 5.89$ . The Lagrangian of Eq. (1.1) should be added with the kinetic and mass terms of the isosinglet  $\omega(782)$  field  $\omega_\mu$ ,

$$\mathcal{L}^{(\omega)} = -\frac{1}{4} (\partial_\mu \omega_\nu - \partial_\nu \omega_\mu)^2 + \frac{m_\omega^2}{2} \omega_\mu^2, \quad (1.4)$$

and the term describing the interaction of  $\omega$  with  $\boldsymbol{\rho}$  and  $\boldsymbol{\pi}$ . The latter comes from the term induced by the anomalous Lagrangian of Wess and Zumino [2,14],

$$\mathcal{L}^{(\omega\rho\pi)} = \frac{N_c g^2}{8\pi^2 f_\pi} \varepsilon_{\mu\nu\lambda\sigma} \partial_\mu \omega_\nu (\boldsymbol{\pi} \cdot \partial_\lambda \boldsymbol{\rho}_\sigma), \quad (1.5)$$

where  $N_c = 3$  is the number of colors, and  $\varepsilon_{\mu\nu\lambda\sigma}$  is the antisymmetric unit tensor. In agreement with Ref. [2], the contribution of the pointlike vertex  $\omega \rightarrow 3\pi$  is omitted. See,

however, the discussion following Eq. (4.10) in Sec. IV where the role of this vertex in the  $\omega \rightarrow 5\pi$  decay is briefly discussed.

The HLS approach [2] permits one to include the axial mesons as well [15]. An ideal treatment would consist of following the line of reasoning that under the assumption of  $m_\rho \sim E \ll m_{a_1}$ , the difference between the models with and without  $a_1$  meson were reduced to the taking into account the higher derivatives [16] expected to be small. In the real life, one has  $m_{a_1}^2 - m_\rho^2 \sim m_\rho^2$ , and the correction may appear to be appreciable even at the  $\rho$  mass. In fact, the calculation [10] shows that the corrections amount to  $\sim 20 - 30\%$  in the width. This means, in particular, that the left shoulder of the  $\rho$  peak, where the contributions of higher derivatives are vanishing rapidly, is the best place to work. In the present paper, we do not take into account the  $a_1$  meson contribution in the  $\rho \rightarrow 4\pi$  decay amplitude. In the meantime, such a contribution is negligible, as will be clear later on, in the  $\omega \rightarrow 5\pi$  decay amplitude.

The rest of the paper is devoted to the working out the consequences of the above Lagrangians for the many pion decays of the  $\rho(770)$  and  $\omega(782)$  mesons. Specifically, the partial widths and resonance excitation curves are calculated for the reactions  $e^+e^- \rightarrow \rho^0 \rightarrow 2\pi^+2\pi^-$  and  $e^+e^- \rightarrow \rho^0 \rightarrow \pi^+\pi^-2\pi^0$ . It is shown that the intensities of the above decays change as fast as two times the phase space variation, upon the energy variation inside the  $\rho$  widths. All this means that  $e^+e^-$  offers an ideal tool for the study of such effects. The decay widths of charged  $\rho$  meson,  $\rho^\pm \rightarrow \pi^\pm 3\pi^0$  and  $\rho^\pm \rightarrow 2\pi^\pm\pi^\mp\pi^0$ , as well as  $\omega$  meson,  $\omega \rightarrow 2\pi^+2\pi^-\pi^0$   $\omega \rightarrow \pi^+\pi^-3\pi^0$ , are also evaluated. We choose these particular modes because the final pions in the decay  $\rho \rightarrow 4\pi$  are practically soft while in the decay  $\omega \rightarrow 5\pi$  they are soft. Note that the final pions in the G-parity violating decay  $\rho \rightarrow 3\pi$  are not sufficiently soft to compare the calculated branching ratio with the predictions of chiral models. The final pions in the decay  $\omega \rightarrow 4\pi$  are sufficiently soft to make such a comparison meaningful. However, the branching ratios of both above G-parity violating decays  $\rho \rightarrow 3\pi$  and  $\omega \rightarrow 4\pi$  are determined completely by the  $\omega\rho$  transition amplitude and by the well known decay  $\omega \rightarrow 3\pi$  and the decay  $\rho \rightarrow 4\pi$ , respectively.

The following material is organized as follows. Section II contains the expressions for the  $\rho \rightarrow 4\pi$  amplitudes. The results of calculation of the excitation curves and partial widths for different isotopic states of four pions are presented in Sec. III. This task is fulfilled in the cases of  $e^+e^-$  annihilation,  $\tau$  decays, and photoproduction. The partial widths of the decays  $\omega \rightarrow 5\pi$  are discussed in Sec. IV. Although an appreciable part of the material of Sec. IV is contained in Ref. [4], we include here the basic results from that paper in order to keep the presentation self-contained. Section V contains concluding remarks. The angular distributions of the various combinations of emitted pions in the decays  $\rho \rightarrow 4\pi$  and  $\omega \rightarrow 5\pi$  obtained for the case of  $e^+e^-$  annihilation are presented in the Appendix.

## II. AMPLITUDES OF $\rho \rightarrow 4\pi$ DECAY

The amplitudes of the decays of our interest are obtained from the Weinberg Lagrangian Eq. (1.1). First, let us obtain the  $\pi \rightarrow 3\pi$  transition amplitudes necessary for the calculation of the many-pion decays of vector mesons. They are given by the diagrams shown in Fig. 1(a) and look as

$$\begin{aligned}
M(\pi^+ \rightarrow \pi_{q_1}^+ \pi_{q_2}^+ \pi_{q_3}^-) &= (1 + P_{12}) \frac{1}{2f_\pi^2} \left\{ -2(q_1, q_2) + a(q_1, q_2 - q_3) \left[ 1 - \frac{m_\rho^2}{D_\rho(q_2 + q_3)} \right] \right\}, \\
M(\pi^+ \rightarrow \pi_{q_1}^+ \pi_{q_2}^0 \pi_{q_3}^0) &= (1 + P_{23}) \frac{1}{2f_\pi^2} \left\{ (q_3, q_1 - 2q_2) + a(q_3, q_1 - q_2) \left[ 1 - \frac{m_\rho^2}{D_\rho(q_1 + q_2)} \right] \right\}, \\
M(\pi^0 \rightarrow \pi_{q_1}^+ \pi_{q_2}^- \pi_{q_3}^0) &= (1 + P_{12}) \frac{1}{2f_\pi^2} \left\{ (q_1, q_2 - 2q_3) - a(q_1, q_2 - q_3) \left[ 1 - \frac{m_\rho^2}{D_\rho(q_2 + q_3)} \right] \right\}, \\
M(\pi^0 \rightarrow \pi_{q_1}^0 \pi_{q_2}^0 \pi_{q_3}^0) &= -\frac{1}{f_\pi^2} [(q_1, q_2) + (q_1, q_3) + (q_2, q_3)].
\end{aligned} \tag{2.1}$$

where  $P_{ij}$  stands for the operator of the interchange of the pion momenta  $q_i$  and  $q_j$ , and

$$D_\rho(q) = m_\rho^2 - q^2 - im_\rho^2 \left( \frac{q^2 - 4m_\pi^2}{m_\rho^2 - 4m_\pi^2} \right)^{3/2} \frac{\Gamma_{\rho\pi\pi}(m_\rho^2)}{\sqrt{q^2}} \tag{2.2}$$

is the inverse propagator of  $\rho$  meson. Our notation for the Lorentz invariant scalar product of two four vectors  $a$  and  $b$  hereafter is  $(a, b) = a_0 b_0 - \mathbf{a} \cdot \mathbf{b}$ . As it will be clear later on, the nonrelativistic expressions for the above amplitudes are needed. They are obtained upon neglecting the space components of the pion four momenta and look as

$$\begin{aligned}
M(\pi^+ \rightarrow \pi_{q_1}^+ \pi_{q_2}^+ \pi_{q_3}^-) &= -\frac{2m_\pi^2}{f_\pi^2}, \\
M(\pi^+ \rightarrow \pi_{q_1}^+ \pi_{q_2}^0 \pi_{q_3}^0) &= -\frac{m_\pi^2}{f_\pi^2}, \\
M(\pi^0 \rightarrow \pi_{q_1}^+ \pi_{q_2}^- \pi_{q_3}^0) &= -\frac{m_\pi^2}{f_\pi^2}, \\
M(\pi^0 \rightarrow \pi_{q_1}^0 \pi_{q_2}^0 \pi_{q_3}^0) &= -\frac{3m_\pi^2}{f_\pi^2}.
\end{aligned} \tag{2.3}$$

Note that the HLS parameter  $a$  drops from the expressions in the nonrelativistic limit.

The diagrams representing the amplitudes of the decays  $\rho \rightarrow 4\pi$  for different combinations of the charges of final pions are shown in Fig. 1(b) and (c). Introducing the four vector of polarization of the decaying  $\rho$  meson  $\varepsilon_\mu$  one can write the general expression for the amplitude in the form

$$M = \frac{g_{\rho\pi\pi}}{f_\pi^2} \varepsilon_\mu J_\mu,$$

where

$$g_{\rho\pi\pi}/f_\pi^2 = \sqrt{a} m_\rho / 2f_\pi^3 \tag{2.4}$$

results from Eq. (1.2). Let us give the expressions for the current  $J_\mu$  for all the decay modes considered here.

(1) The decay  $\rho^0(q) \rightarrow \pi^+(q_1)\pi^+(q_2)\pi^-(q_3)\pi^-(q_4)$ . One has

$$J_\mu = (1 + P_{12})(1 + P_{34}) \left\{ -q_{1\mu} \left[ \frac{1}{2} + \frac{a(q_2, q_3) - (a-2)(q_3, q_4)}{D_\pi(q - q_1)} \right] \right\}$$

$$\begin{aligned}
& +q_{3\mu} \left[ \frac{1}{2} + \frac{a(q_1, q_4) - (a-2)(q_1, q_2)}{D_\pi(q - q_3)} \right] \\
& + am_\rho^2 (1 + P_{13}) \frac{q_{1\mu}(q_3, q_2 - q_4)}{D_\pi(q - q_1) D_\rho(q_2 + q_4)} \Bigg\}. \tag{2.5}
\end{aligned}$$

Hereafter  $D_\pi(q) = m_\pi^2 - q^2$  is the inverse propagator of pion.

(2) The decay  $\rho^0(q) \rightarrow \pi^+(q_1)\pi^-(q_2)\pi^0(q_3)\pi^0(q_4)$ . In this case one has  $J_\mu = J_\mu^{\text{nan}} + J_\mu^{\text{an}}$ , where

$$\begin{aligned}
J_\mu^{\text{nan}} = & -(1 - P_{12})(1 + P_{34})q_{1\mu} \left\{ \frac{1}{4} + \frac{1}{D_\pi(q - q_1)} [(a-1)(q_3, q_4) - (a-2)(q_2, q_3) \right. \\
& \left. + am_\rho^2 \frac{(q_3, q_2 - q_4)}{D_\rho(q_2 + q_4)}] \right\} \\
& + (1 + P_{34}) \frac{m_\rho^2}{2D_\rho(q_1 + q_3)D_\rho(q_2 + q_4)} [(q_1 + q_3 - q_2 - q_4)_\mu (q_1 - q_3, q_2 - q_4) \\
& - 2(q_1 - q_3)_\mu (q_1 + q_3, q_2 - q_4) + 2(q_2 - q_4)_\mu (q_2 + q_4, q_1 - q_3)] \tag{2.6}
\end{aligned}$$

is obtained from Eq. (1.1), while the contribution of the term induced by the anomalous Lagrangian of Wess and Zumino [2,14] manifesting in the process  $\rho^0 \rightarrow \omega\pi^0 \rightarrow \pi^+\pi^-\pi^0\pi^0$ , is given by the expression

$$\begin{aligned}
J_\mu^{\text{an}} = & 2 \left( \frac{N_c g^2}{8\pi^2} \right)^2 (1 + P_{34}) [q_{1\mu}(1 - P_{23})(q, q_2)(q_3, q_4) \\
& + q_{2\mu}(1 - P_{13})(q, q_3)(q_1, q_4) + q_{3\mu}(1 - P_{12})(q, q_1)(q_2, q_4)] \\
& \times \left[ \frac{1}{D_\rho(q_1 + q_2)} + \frac{1}{D_\rho(q_1 + q_3)} + \frac{1}{D_\rho(q_2 + q_3)} \right] \frac{1}{D_\omega(q - q_4)}, \tag{2.7}
\end{aligned}$$

where  $D_\omega(q) = m_\omega^2 - q^2$  is the inverse  $\omega$  meson propagator. In general, this term is attributed to the contribution of higher derivatives. Nevertheless, we take it into account to show the effect of the latter and the dynamical effect of the opening of the channel  $\rho \rightarrow \omega\pi \rightarrow 4\pi$ . The following amplitudes of the charged  $\rho$  decay are necessary for obtaining the  $\omega \rightarrow 5\pi$  decay amplitude, and are of their own interest when studying the reactions of peripheral  $\rho$  meson production and  $\tau$  decays.

(3) The decay  $\rho^+(q) \rightarrow \pi^+(q_1)\pi^0(q_2)\pi^0(q_3)\pi^0(q_4)$ . One has

$$\begin{aligned}
J_\mu = & (1 + P_{24} + P_{34}) \left\{ 2q_{1\mu} \left[ \frac{1}{3} + \frac{(q_2, q_3)}{D_\pi(q - q_1)} \right] - \frac{q_{4\mu}}{D_\pi(q - q_4)} [2(a-1)(q_2, q_3) \right. \\
& \left. - (a-2)(q_1, q_2 + q_3) + am_\rho^2 (1 + P_{23}) \frac{(q_2, q_1 - q_3)}{D_\rho(q_1 + q_3)}] \right\}. \tag{2.8}
\end{aligned}$$

(4) The decay  $\rho^+(q) \rightarrow \pi^+(q_1)\pi^+(q_2)\pi^-(q_3)\pi^0(q_4)$ . Here, the contribution induced by the anomalous Lagrangian of Wess and Zumino is also possible, hence  $J_\mu = J_\mu^{\text{nan}} + J_\mu^{\text{an}}$ , where

$$J_\mu^{\text{nan}} = (1 + P_{12}) \left\{ \frac{1}{2}(q_1 - q_4)_\mu + \frac{q_{1\mu}(1 + P_{23})}{D_\pi(q - q_1)} [(a-1)(q_2, q_3) - (a-2)(q_2, q_4)] \right\}$$

$$\begin{aligned}
& -\frac{q_{4\mu}}{D_\pi(q-q_4)} [a(q_1, q_3) - (a-2)(q_1, q_2)] \\
& -am_\rho^2 \left[ \frac{q_{1\mu}}{D_\pi(q-q_1)} (1+P_{23}) \frac{(q_2, q_3-q_4)}{D_\rho(q_3+q_4)} + \frac{q_{4\mu}(q_1, q_2-q_3)}{D_\pi(q-q_4)D_\rho(q_2+q_3)} \right] \\
& + \frac{m_\rho^2}{2D_\rho(q_1+q_3)D_\rho(q_2+q_4)} [(q_1+q_3-q_2-q_4)_\mu(q_1-q_3, q_2-q_4) \\
& -2(q_1-q_3)_\mu(q_1+q_3, q_2-q_4) + 2(q_2-q_4)_\mu(q_1-q_3, q_2+q_4)] \} \tag{2.9}
\end{aligned}$$

is obtained from Eq. (1.1), while the term induced by the anomaly looks as

$$\begin{aligned}
J_\mu^{\text{an}} &= 2 \left( \frac{N_c g^2}{8\pi^2} \right)^2 (1+P_{23}) [q_{1\mu}(1-P_{24})(q, q_4)(q_2, q_4) \\
& + q_{2\mu}(1-P_{14})(q, q_1)(q_3, q_4) + q_{4\mu}(1-P_{12})(q, q_2)(q_1, q_3)] \\
& \times \left[ \frac{1}{D_\rho(q_1+q_2)} + \frac{1}{D_\rho(q_1+q_4)} + \frac{1}{D_\rho(q_2+q_4)} \right] \frac{1}{D_\omega(q-q_3)}. \tag{2.10}
\end{aligned}$$

One can verify that up to the corrections of the order of  $\sim m_\pi^2/m_\rho^2$ , the above written amplitudes vanish in the limit of vanishing 4-momentum of each final pion. In other words, they obey the Adler condition.

It is useful to obtain the nonrelativistic expressions for the  $\rho \rightarrow 4\pi$  decay amplitudes which are relevant for the four pion invariant mass below 700 MeV. This can be made upon neglecting the space components of the pion momenta. One can convince oneself that  $a$  enters the expressions for amplitudes as an overall factor Eq. (2.4) in this limit, so that the latter look as

$$\begin{aligned}
M(\rho^0 \rightarrow \pi_{q_1}^+ \pi_{q_2}^+ \pi_{q_3}^- \pi_{q_4}^-) &\simeq -\frac{g_{\rho\pi\pi}}{2f_\pi^2}(\varepsilon, q_1 + q_2 - q_3 - q_4), \\
M(\rho^0 \rightarrow \pi_{q_1}^+ \pi_{q_2}^- \pi_{q_3}^0 \pi_{q_4}^0) &\simeq -\frac{g_{\rho\pi\pi}}{4f_\pi^2}(\varepsilon, q_1 - q_2), \\
M(\rho^+ \rightarrow \pi_{q_1}^+ \pi_{q_2}^0 \pi_{q_3}^0 \pi_{q_4}^0) &\simeq \frac{g_{\rho\pi\pi}}{f_\pi^2}(\varepsilon, q_1), \\
M(\rho^+ \rightarrow \pi_{q_1}^+ \pi_{q_2}^+ \pi_{q_3}^- \pi_{q_4}^0) &\simeq \frac{g_{\rho\pi\pi}}{4f_\pi^2}(\varepsilon, q_1 + q_2 - 2q_4). \tag{2.11}
\end{aligned}$$

The amplitudes of the four pion decays of the  $\rho^-$  are obtained from corresponding expressions for the  $\rho^+$  by reversing an overall sign. These considerably simplified expressions are especially convenient in the calculation of the  $\omega \rightarrow 5\pi$  decay amplitude, because the typical invariant masses of the four pion system in the above decay are in the vicinity of 620 MeV (see Sec. IV for more detail).

### III. RESULTS FOR VARIOUS $\rho \rightarrow 4\pi$ DECAYS

When evaluating the partial widths of the  $4\pi$  decays of  $\rho$  meson the modulus squared of the matrix element is expressed via the Kumar variables [17]. The idea of speeding up the numerical integration suggested in Ref. [18] is realized in the numerical algorithm.

The results of evaluation of the partial widths at  $\sqrt{s} = m_\rho = 770$  MeV are as follows:  $\Gamma(\rho^0 \rightarrow 2\pi^+2\pi^-, m_\rho) = 0.89$  keV,  $\Gamma(\rho^0 \rightarrow \pi^+\pi^-2\pi^0, m_\rho) = 0.24$  and  $0.44$  keV, respectively, without and with the induced anomaly term being taken into account. This coincides with the results obtained in Ref. [10]. In the case of the charged  $\rho$  meson decays it is obtained for the first time:  $\Gamma(\rho^+ \rightarrow \pi^+3\pi^0, m_\rho) = 0.41$  keV,  $\Gamma(\rho^+ \rightarrow 2\pi^+\pi^-\pi^0, m_\rho) = 0.71$  and  $0.90$  keV respectively, without and with the anomaly induced term being taken into account. When obtaining these figures, the narrow  $\rho$  width approximation is used. This is equivalent to the setting  $\Gamma_{\rho\pi\pi} \rightarrow 0$  in Eq. (2.2). Keeping the physical value of the  $\rho$  width gives the results deviating from those obtained in the narrow width approximation by a quantity that does not exceed a few percents of the values obtained in the latter. This is true in the case of the invariant mass of the four pion state lying below the  $\rho\pi$  threshold energy,  $m_{4\pi} < 910$  MeV. Recall that the allowing for the finite widths effects is in fact equivalent to the loop correction being taken into account.

The above results are obtained at  $a = 2$ . The variation of  $a$  within 20% around this value implies the variation of the branching ratios within 20% around the values cited above. This fact can be easily traced in the nonrelativistic limit where the parameter  $a$  enters the expressions for the amplitudes as an overall factor  $\sqrt{a}$ , see Eqs. (1.2) and (2.11).

### A. The decay $\rho^0 \rightarrow 4\pi$ as manifested in $e^+e^-$ annihilation.

The results of the evaluation of the  $4\pi$  state production cross section in the reaction  $e^+e^- \rightarrow \rho^0 \rightarrow 4\pi$

$$\sigma_{e^+e^- \rightarrow \rho \rightarrow 4\pi}(s) = \frac{12\pi m_\rho^3 \Gamma_{\rho e^+e^-}(m_\rho) \Gamma_{\rho \rightarrow 4\pi}(E)}{E^3 |D_\rho(s)|^2}, \quad (3.1)$$

where  $s = E^2$  is the square of the total center-of mass energy, and  $D_\rho(s)$  is obtained from Eq. (2.2) upon the substitution  $q^2 \rightarrow s$ , are plotted in Figs. 2 and 3. Note that the values of the vector meson parameters taken from Ref. [19] are used hereafter. The following notations are such that

$$q(m_a, m_b, m_c) = \frac{1}{2m_a} \lambda^{1/2}(m_a^2, m_b^2, m_c^2), \quad (3.2)$$

with the function  $\lambda$  given by the equation

$$\lambda(x, y, z) = x^2 + y^2 + z^2 - 2(xy + xz + yz), \quad (3.3)$$

is the momentum of final particle  $b$  (or  $c$ ) in the rest frame system of decaying particle  $a$ .

To demonstrate the effects of chiral dynamics, also shown is the energy dependence of the cross section evaluated in the model of pure phase space for the four pion decay. In this model, the  $4\pi$  partial width normalized to the width at the  $\rho$  mass calculated in the dynamical model, is given by the expression

$$\Gamma^{\text{LIPS}}(\rho \rightarrow 4\pi, s) = \Gamma(\rho \rightarrow 4\pi, m_\rho^2) \frac{W_{4\pi}(s)}{W_{4\pi}(m_\rho^2)}, \quad (3.4)$$

where the four pion phase space volume is [17,20]



$$\begin{aligned}
W_{4\pi}(s) &= \frac{\pi^3}{16(2\pi)^8 s^{3/2} N_s} \int_{(3m_\pi)^2}^{(\sqrt{s}-m_\pi)^2} \frac{ds_1}{s_1} \lambda^{1/2}(s, s_1, m_\pi^2) \\
&\times \int_{(2m_\pi)^2}^{(\sqrt{s_1}-m_\pi)^2} \frac{ds_2}{s_2} \lambda^{1/2}(s_1, s_2, m_\pi^2) \\
&\times \lambda^{1/2}(s_2, m_\pi^2, m_\pi^2).
\end{aligned} \tag{3.5}$$

In the above formula,  $N_s = 4$  (2) is the factor that takes into account the identity of final pions in the final state  $2\pi^+2\pi^-$  ( $\pi^+\pi^-2\pi^0$ ), respectively. As the evaluation shows, the ratio

$$R(s) = \Gamma(\rho \rightarrow 2\pi^+2\pi^-, s) / \Gamma^{\text{LIPS}}(\rho \rightarrow 2\pi^+2\pi^-, s)$$

changes from 0.4 at  $\sqrt{s} = 650$  MeV to 1 at  $\sqrt{s} = m_\rho$ . As can be observed from the figures, the rise of the  $\rho \rightarrow 4\pi$  partial width with the energy increase is such fast that it compensates completely the falling of the  $\rho$  meson propagator and electronic width. Also noticeable is the dynamical effect of the  $\omega\pi^0$  production threshold in the decay  $\rho^0 \rightarrow \pi^+\pi^-2\pi^0$  at  $\sqrt{s} > 850$  MeV which results from the anomaly induced Lagrangian, see Fig. 3. To quantify the above-mentioned effect of vanishing contribution of higher derivatives at the left shoulder of the  $\rho$  resonance it should be noted that the difference between magnitude of  $\Gamma(\rho \rightarrow \pi^+\pi^-2\pi^0, s)$  with and without the term originating from the anomaly induced Lagrangian, equal to 100% at  $\sqrt{s} = m_\rho$ , diminishes rapidly with the energy decrease amounting to 8% at  $\sqrt{s} = 700$  MeV and 0.3% at  $\sqrt{s} = 650$  MeV. It should be pointed out that the evaluation of the partial widths with the nonrelativistic expressions for the  $\rho \rightarrow 4\pi$  amplitudes, Eq. (2.11), gives the values which deviate from those obtained with the exact expressions, by the quantity ranging from 7 to 15 %, depending on the energy in the interval from 610 to 770 MeV.

As is seen from Fig. 2, the predictions of chiral symmetry for the  $e^+e^- \rightarrow 2\pi^+2\pi^-$  reaction cross section do not contradict to the three lowest experimental points of CMD-2 detector [21]. However, at  $\sqrt{s} > 800$  MeV one can observe a substantial deviation between the predictions of the Lagrangian (1.1) and the data of CMD-2. In all appearance, this is due to the contribution of higher derivatives and chiral loops neglected in the present work. It is expected that the left shoulder of the  $\rho$  is practically free of such contributions, and by this reason it is preferable for studying the dynamical effects of chiral symmetry. Note that even at  $\sqrt{s} = 650$  MeV, where the contribution of higher derivatives is negligible, one can hope to gather one event of the reaction  $e^+e^- \rightarrow 2\pi^+2\pi^-$  per day, and up to 10 events of this reaction per day at  $\sqrt{s} = 700$  MeV, provided the luminosity  $L = 10^{32}\text{cm}^{-2}\text{s}^{-1}$  is achieved, i.e. to have a factory for a comprehensive study of the chiral dynamics of many-pion systems.

Due to helicity conservation,  $\rho$  meson is produced in the states with the spin projections  $\lambda = \pm 1$  on the  $e^+e^-$  beam axes characterized by the unit vector  $\mathbf{n}_0$ . The latter is assumed to be directed along the z axes. Then, using the expressions for the total  $\rho \rightarrow 4\pi$  amplitudes, one can obtain the angular distributions for the final pions. They are expected to be cumbersome. However, the good approximation for these distributions are obtained from the approximate nonrelativistic expression Eq. (2.11). The specific formulas are collected in the Appendix.

### B. $\rho \rightarrow 4\pi$ in $\tau$ decays

Based on the vector current conservation, the partial width of the decay  $\tau^- \rightarrow \nu_\tau(4\pi)^-$  [22,23] can be written as the integral over the invariant mass of the four pion state  $m$ , extended up to some mass  $m_0$ , whose maximal value is  $m_{0\max} = m_\tau$ :

$$B_{\tau^- \rightarrow \nu_\tau(4\pi)^-}(m_0) = T_\tau \int_{4m_\pi}^{m_0} dm \frac{2m^2 \Gamma_{\tau^- \rightarrow \nu_\tau \rho^-}(m)}{\pi |D_\rho(m^2)|^2} \times \Gamma_{\rho^- \rightarrow (4\pi)^-}(m), \quad (3.6)$$

where  $T_\tau$  and

$$\Gamma_{\tau^- \rightarrow \nu_\tau \rho^-}(m) = \frac{G_F^2 \cos^2 \theta_C}{8\pi f_\rho^2} m_\tau^3 m_\rho^2 \left(1 - \frac{m^2}{m_\tau^2}\right)^2 \times \left(1 + 2\frac{m^2}{m_\tau^2}\right) \quad (3.7)$$

are, respectively, the lifetime of  $\tau$  lepton and its partial width of the decay  $\tau^- \rightarrow \nu_\tau \rho^-$  [22], with  $m$  being the invariant mass of the four pion state. Using the numerical values of the  $\rho \rightarrow 4\pi$  decay widths, one can evaluate the branching ratios of the four pion  $\tau$  decays for various values of the upper invariant mass  $m_0$  of the latter. The results of the evaluation of the branching ratios of the decays  $\tau^- \rightarrow \nu_\tau 2\pi^- \pi^+ \pi^0$  and  $\tau^- \rightarrow \nu_\tau \pi^- 3\pi^0$  for the values of the invariant mass of the four pion system from 600 to 850 MeV are plotted in Figs. 4 and 5, respectively. In particular, taking  $m_0 = 740$  MeV one obtains

$$B(\tau^- \rightarrow \nu_\tau 2\pi^- \pi^+ \pi^0, 740\text{MeV}) = \begin{cases} 7.6 \times 10^{-8} & (\text{without anomaly induced term}) \\ 8.4 \times 10^{-8} & (\text{with anomaly induced term}) \end{cases}, \quad (3.8)$$

and

$$B(\tau^- \rightarrow \nu_\tau 3\pi^0 \pi^-, 740\text{MeV}) = 4.6 \times 10^{-8}. \quad (3.9)$$

Corresponding values for the upper integration mass  $m_0 = 640$  MeV are

$$B(\tau^- \rightarrow \nu_\tau 2\pi^- \pi^+ \pi^0, 640\text{MeV}) = \begin{cases} 2.895 \times 10^{-10} & (\text{without anomaly induced term}) \\ 2.900 \times 10^{-10} & (\text{with anomaly induced term}) \end{cases}, \quad (3.10)$$

and

$$B(\tau^- \rightarrow \nu_\tau 3\pi^0 \pi^-, 640\text{MeV}) = 1.8 \times 10^{-10}. \quad (3.11)$$

The comparison of Eqs. (3.8) and (3.10), and both curves in Fig. 4 again demonstrates that the contributions of higher derivatives represented by the terms induced by the anomalous Lagrangian of Wess and Zumino vanish rapidly with the decreasing of mass. Unfortunately, the domains in the low four pion invariant mass where the effects of chiral dynamics are clean, are hardly accessible with  $\tau$  factories. Indeed, guided by the expression for the cross section of the  $\tau$  lepton pair production in  $e^+e^-$  annihilation

$$\sigma_{\tau+\tau^-}(s) = \frac{4\pi\alpha^2}{3s} \sqrt{1 - \frac{4m_\tau^2}{s}} \left(1 + 2\frac{m_\tau^2}{s}\right), \quad (3.12)$$

one can find that up to  $N = 25 \times 10^7$   $\tau$  lepton pairs with the total energy  $\sqrt{s} = m_{\psi(2S)}$  can be produced per season at  $\tau$ -charm factory with expected luminosity  $L = 10^{34} \text{ cm}^{-2} \text{ s}^{-1}$  [19]. This implies that one can detect only from 2 to 4 events per season in the four pion mass range below 700 MeV. Nevertheless, the event counting rate rises rapidly with the increase of the upper integration mass  $m_0$  in Eq. (3.6), reaching, at  $m_0 = m_\rho$ , the figure about 60 to 120 events per season, depending on the charge combination of the final pions.

### C. The decay $\rho \rightarrow 4\pi$ in photoproduction, $\pi N \rightarrow \rho\pi N$ , and so on.

To characterize the possibility of the study of the  $\rho \rightarrow 4\pi$  decays in photoproduction, we calculate the quantity

$$B_{\rho \rightarrow 4\pi}^{\text{aver}}(m_0) = \frac{2}{\pi} \int_{4m_\pi}^{m_0} dm \frac{m^2 \Gamma_{\rho \rightarrow 4\pi}(m)}{|D_\rho(m^2)|^2}, \quad (3.13)$$

which is the average of the branching ratio over the invariant mass of the four pion state. In the limit  $m_0 \rightarrow \infty$ , Eq. (3.13) serves as the definition of the branching ratio in case of a wide resonance. Equation (3.13) should be confronted with the familiar definition of the branching ratio at the  $\rho$  mass

$$B_{\rho \rightarrow 4\pi}(m_\rho) = \Gamma_{\rho \rightarrow 4\pi} / \Gamma_\rho, \quad (3.14)$$

which results from Eq. (3.13) upon the replacement  $m\Gamma_\rho/\pi|D_\rho(m^2)|^2 \rightarrow \delta(m^2 - m_\rho^2)$  valid in the limit of narrow width. With the partial widths evaluated here one finds

$$B_{\rho^0 \rightarrow 2\pi^+ 2\pi^-}(m_\rho) = 5.9 \times 10^{-6}, \quad (3.15)$$

and

$$B_{\rho^0 \rightarrow \pi^+ \pi^- 2\pi^0}(m_\rho) = \begin{cases} 1.6 \times 10^{-6} & (\text{without anomaly induced term}) \\ 2.9 \times 10^{-6} & (\text{with anomaly induced term}) \end{cases}. \quad (3.16)$$

The results of plotting the quantity  $B_{\rho \rightarrow 4\pi}^{\text{aver}}(m_0)$  are shown in Fig. 6 and 7. In particular, the evaluation gives  $B_{\rho^0 \rightarrow 2\pi^+ 2\pi^-}^{\text{aver}}(m_0) = 4.4 \times 10^{-6}$ ,  $6.1 \times 10^{-8}$ , and  $1.4 \times 10^{-9}$  at  $m_0 = 850$ , 700, and 640 MeV, respectively. In the case of other four pion decay mode of the  $\rho^0$  the results are the following. In the model with the vanishing term induced by the anomalous Lagrangian of Wess and Zumino one obtains  $B_{\rho^0 \rightarrow \pi^+ \pi^- 2\pi^0}^{\text{aver}}(m_0) = 1.3 \times 10^{-6}$ ,  $1.58 \times 10^{-8}$ , and  $3.66 \times 10^{-10}$  at  $m_0 = 850$ , 700, and 640 MeV. In the model that includes the above term, one obtains  $B_{\rho^0 \rightarrow \pi^+ \pi^- 2\pi^0}^{\text{aver}}(m_0) = 4.9 \times 10^{-6}$ ,  $1.65 \times 10^{-8}$ , and  $3.63 \times 10^{-10}$  at the same respective values of  $m_0$ . As is expected, the branching ratios in the two mentioned models converge to each other in view of the rapid vanishing of the contributions due to the terms with higher derivatives. The difference between the two definitions of the branching ratio is seen upon comparison of  $B_{\rho \rightarrow 4\pi}^{\text{aver}}(m_0 = 850 \text{ MeV})$  evaluated for various charge combinations of the final pions, with Eqs. (3.15) and (3.16).

With the total number of  $\rho$  mesons  $N \simeq 6 \times 10^9$  expected to be produced on nucleon at the Jefferson Laboratory "photon factory" [24] one may hope to observe about 100, 360 events of the  $\rho$  decays into the states  $\pi^+\pi^-2\pi^0$ ,  $2\pi^+2\pi^-$ , respectively, in the mass range  $m_0 < 700$  MeV where the effects of chiral dynamics are most clean. The photoproduction on heavy nuclei results in increasing the number of produced  $\rho$  mesons faster than  $A^{2/3}$ , where  $A$  is the atomic weight. A generally adopted behavior is in accord with the behavior  $A^{0.8-0.95}$  [25]. Thus the photoproduction of the four pion states on heavy nuclei would give the possibility of the high statistics study of the effects of chiral dynamics in the four pion decays of the  $\rho(770)$ . It should be recalled once more that the counting rate rises rapidly with the increase of  $m_0$ .

The conclusions about the angular distributions of the final pions with zero net charge in photoproduction are the following. Of course, their general expression should be deduced from the full decay amplitudes which can be found in Sec. II, together with the detailed form of the photoproduction mechanism. The qualitative picture, however, can be obtained upon assuming  $s$ -channel helicity conservation to be a good selection rule for the photoproduction reactions [25,26]. Then in the helicity reference frame characterized as the frame where the  $\rho$  is at rest, while its spin quantization axes is directed along the  $\rho$  momentum in the center-of-mass system, the expressions for the angular distributions coincide with the corresponding expressions for the production of these states in  $e^+e^-$  annihilation that can be found in the Appendix. Since, at high energies, the direction of the final  $\rho$  momentum lies at the scattering angle less than  $0.5^\circ$  in the case of the photoproduction on heavy nuclei, the vector  $\mathbf{n}_0$  can be treated as pointed along the photon beam direction.

Note that another peripheral reactions can provide a sufficiently intense source of  $\rho$  mesons. For example, the diffractive production of the  $\rho\pi$  state in  $\pi N$  collisions are currently under study with the VES detector in Protvino. The regions of the four pion invariant mass spectrum larger than  $m_\rho$ , namely,  $m_0 \simeq 850$  MeV where  $B^{\text{aver}}(\rho \rightarrow 4\pi, m_0) \sim 10^{-5}$  should be included to measure the  $\rho \rightarrow 4\pi$  branching ratio reliably. As is explained in Introduction, this would require the inclusion of the contributions of  $a_1$  meson and higher derivatives to the total amplitude. Nevertheless, the results of the present paper shown in Figs. 8 and 9, obtained upon neglecting the latter contributions can be regarded as a guess in the experimental work in this direction.

#### IV. THE DECAY $\omega \rightarrow 5\pi$

One may convince oneself that the  $\omega \rightarrow \rho\pi \rightarrow 5\pi$  decay amplitude unambiguously results from the anomaly induced Lagrangian (1.5). This amplitude is represented by the diagrams shown in Fig. 10. As one can foresee, its general expression looks cumbersome. However, it can be considerably simplified upon noting that due to the low pion momentum,  $|\mathbf{q}_\pi| \simeq 0.5m_\pi$ , the nonrelativistic expressions Eq. (2.11) for the  $\rho \rightarrow 4\pi$  decay amplitudes in the diagrams Fig. 10(a) are valid with the accuracy 5% in the  $4\pi$  mass range relevant for the present purpose [3]. This accuracy is estimated from the direct evaluation of the  $\rho \rightarrow 4\pi$  branching ratios with the exact  $\rho \rightarrow 4\pi$  decay formulas given in Sec. II, and with the approximate ones, Eq. (2.11). The evaluation shows that the results differ by approximately 10 % in the width. Likewise, the expression for the combination  $D_\pi^{-1}M(\pi \rightarrow 3\pi)$  standing in the expression for the diagrams in Fig. 10(b) can be replaced, with the same accuracy, by

$-(8m_\pi^2)^{-1}$  times the nonrelativistic  $\pi \rightarrow 3\pi$  amplitudes in Eq. (2.3). First, using Eq. (2.11) one obtains the expression for the sum of the diagrams shown in Fig. 10(a). Second, using Eq. (2.3), one obtains the expression for the sum of the diagrams shown in Fig. 10(b). Note that the contribution of the diagrams Fig. 10(b) was neglected in Ref. [3]. The final expressions for the  $\omega \rightarrow 5\pi$  decay amplitudes, upon neglecting the terms of the order of  $O(|\mathbf{q}_\pi^4/m_\pi^4|)$  or higher, can be represented in the form:

$$\begin{aligned}
M(\omega \rightarrow 2\pi^+2\pi^-\pi^0) = & \frac{N_c g_{\rho\pi\pi} g^2}{8(2\pi)^2 f_\pi^3} \varepsilon_{\mu\nu\lambda\sigma} q_\mu \epsilon_\nu \left\{ (1 + P_{12}) q_{1\lambda} \left[ \frac{(q_2 + 3q_4)_\sigma}{D_\rho(q - q_1)} - \frac{2q_{4\sigma}}{D_\rho(q_1 + q_4)} \right] \right. \\
& - (1 + P_{35}) q_{3\lambda} \left[ \frac{(q_5 + 3q_4)_\sigma}{D_\rho(q - q_3)} - \frac{2q_{4\sigma}}{D_\rho(q_3 + q_4)} \right] \\
& \left. - (1 + P_{12})(1 + P_{35}) q_{3\lambda} \left[ \frac{2q_{4\sigma}}{D_\rho(q - q_4)} + \frac{q_{1\sigma}}{D_\rho(q_1 + q_3)} \right] \right\}, \quad (4.1)
\end{aligned}$$

with the final momentum assignment according to  $\pi^+(q_1)\pi^+(q_2)\pi^-(q_3)\pi^-(q_5)\pi^0(q_4)$ , and

$$\begin{aligned}
M(\omega \rightarrow \pi^+\pi^-\pi^0) = & \frac{N_c g_{\rho\pi\pi} g^2}{8(2\pi)^2 f_\pi^3} (1 - P_{12})(1 + P_{34} + P_{35}) \varepsilon_{\mu\nu\lambda\sigma} q_\mu \epsilon_\nu q_{1\lambda} \\
& \times \left\{ q_{3\sigma} \left[ \frac{1}{D_\rho(q - q_3)} - \frac{1}{D_\rho(q_1 + q_3)} \right] \right. \\
& \left. - q_{2\sigma} \left[ \frac{4}{3D_\rho(q - q_1)} - \frac{1}{2D_\rho(q_1 + q_2)} \right] \right\}, \quad (4.2)
\end{aligned}$$

with the final momentum assignment according to  $\pi^+(q_1)\pi^-(q_2)\pi^0(q_3)\pi^0(q_4)\pi^0(q_5)$ . In both above formulas,  $\epsilon_\nu$ ,  $q_\mu$  stand for four-vectors of polarization and momentum of  $\omega$  meson. Note that the first term in each square bracket refers to the specific diagram shown in Fig. 10(a) while the second one does to the diagram shown in Fig. 10(b).

Yet even in this simplified form the expressions for the  $\omega \rightarrow 5\pi$  amplitudes are not easy to use for evaluation of the branching ratios. To go further, one should note the following. One can check that the invariant mass of the  $4\pi$  system on which the contribution of the diagrams shown in Fig. 10(a) depends, changes in the very narrow range  $558 \text{ MeV} < m_{4\pi} < 642 \text{ MeV}$ . Hence, one can set it in all the  $\rho$  propagators standing as the first terms in all square brackets in Eqs. (4.2) and (4.1), with the accuracy 20% in width, to the "equilibrium" value  $\overline{m_{4\pi}^2}^{-1/2} = 620 \text{ MeV}$  evaluated for the pion energy  $E_\pi = m_\omega/5$  which gives the dominant contribution. The same is true for the invariant mass of the pion pairs on which the  $\rho$  propagators standing as the last terms in square brackets of the above expressions, depend. This invariant mass varies in the narrow range  $280 \text{ MeV} < m_{2\pi} < 360 \text{ MeV}$ . With the same accuracy, one can set it to  $\overline{m_{2\pi}^2}^{-1/2} = 295 \text{ MeV}$  in all relevant propagators. On the other hand, the amplitude of the process  $\omega \rightarrow \rho^0\pi^0 \rightarrow (2\pi^+2\pi^-\pi^0)$  is

$$\begin{aligned}
M[\omega \rightarrow \rho^0\pi^0 \rightarrow (2\pi^+2\pi^-\pi^0)] = & 4 \frac{N_c g_{\rho\pi\pi} g^2}{8(2\pi)^2 f_\pi^3} \\
& \times \varepsilon_{\mu\nu\lambda\sigma} q_\mu \epsilon_\nu (q_1 + q_2)_\lambda \\
& \times \frac{q_{4\sigma}}{D_\rho(q - q_4)}, \quad (4.3)
\end{aligned}$$

where the momentum assignment is the same as in Eq. (4.1). The other relevant amplitude corresponding to the first diagram in Fig. 10(b) is

$$M[\omega \rightarrow \rho^0 \pi^0 \rightarrow (\pi^+ \pi^-)(\pi^+ \pi^- \pi^0)] = \frac{N_c g_{\rho\pi\pi} g^2}{8(2\pi)^2 f_\pi^3} \varepsilon_{\mu\nu\lambda\sigma} q_\mu \epsilon_\nu \times (1 + P_{12})(1 + P_{35}) \frac{q_{1\lambda} q_{3\sigma}}{D_\rho(q_1 + q_3)} \quad (4.4)$$

Taking into account the above consideration concerning the invariant masses, one can replace all the  $\rho$  propagators standing as the first terms in square parentheses of Eq. (4.1) with  $1/D_\rho(q - q_4)$  one. In the same manner, all the  $\rho$  propagators standing as the second terms in square parentheses can be replaced with  $1/D_\rho(q_1 + q_3)$ . Then the comparison of Eqs. (4.1), (4.3), and (4.4) shows that

$$M(\omega \rightarrow 2\pi^+ 2\pi^- \pi^0) \approx \frac{5}{2} M[\omega \rightarrow \rho^0 \pi^0 \rightarrow (2\pi^+ 2\pi^-) \pi^0] \times \left[ 1 - \frac{D_\rho(\overline{m_{4\pi}^2})}{2D_\rho(\overline{m_{2\pi}^2})} \right], \quad (4.5)$$

where we replace the ratio  $D_\rho(q - q_4)/D_\rho(q_1 + q_3)$  with the ratio  $D_\rho(\overline{m_{4\pi}^2})/D_\rho(\overline{m_{2\pi}^2})$  evaluated at the "equilibrium" point. The same treatment shows that

$$M(\omega \rightarrow \pi^+ \pi^- 3\pi^0) \approx \frac{5}{2} M[\omega \rightarrow \rho^+ \pi^- \rightarrow (\pi^+ 3\pi^0) \pi^-] \times \left[ 1 - \frac{D_\rho(\overline{m_{4\pi}^2})}{2D_\rho(\overline{m_{2\pi}^2})} \right], \quad (4.6)$$

where

$$M[\omega \rightarrow \rho^+ \pi^- \rightarrow (\pi^+ 3\pi^0) \pi^-] = -4 \frac{N_c g_{\rho\pi\pi} g^2}{8(2\pi)^2 f_\pi^3} \times \frac{\varepsilon_{\mu\nu\lambda\sigma} q_\mu \epsilon_\nu q_{1\lambda} q_{2\sigma}}{D_\rho(q - q_2)}, \quad (4.7)$$

and the final momenta assignment is the same as in Eq. (4.2). The numerical values of  $\overline{m_{4\pi}^2}^{-1/2}$  and  $\overline{m_{2\pi}^2}^{-1/2}$  found above are such that the correction factor in parentheses of Eqs. (4.5) and (4.6) amounts to 20% in magnitude. In what follows, the above correction will be taken into account as an overall factor of 0.64 in front of the branching ratios of the decays  $\omega \rightarrow 5\pi$ . When making this estimate, the imaginary part of the  $\rho$  propagators in square brackets of Eq. (4.5) and (4.6) is neglected. This assumption is valid with the accuracy better than 1% in width.

The evaluation of the partial widths valid with the accuracy 20% can be obtained upon using the expressions (4.3)- (4.7). Such an accuracy is estimated by noting that the numerical magnitude of the  $\rho$  propagators in the expressions for the  $\omega \rightarrow 5\pi$  decay amplitudes in Eqs. (4.1) and (4.2) evaluated by assuming the invariant mass of the four pion system to be determined by either the "equilibrium" pion energy or by the center of allowed range of

the variation of this mass, respectively, differs by the quantity not exceeding 10 % of the numerical value of the  $\rho$  propagator. Defining the branching ratio at the  $\omega$  mass as

$$B_{\omega \rightarrow 5\pi} = \Gamma_{\omega \rightarrow 5\pi} / \Gamma_{\omega}, \quad (4.8)$$

one finds

$$\begin{aligned} B_{\omega \rightarrow 2\pi^+ 2\pi^- \pi^0} &= \left| 1 - \frac{D_{\rho}(\overline{m_{4\pi}^2})}{2D_{\rho}(\overline{m_{2\pi}^2})} \right|^2 \left( \frac{5}{2} \right)^2 \frac{2}{\pi \Gamma_{\omega}} \\ &\quad \times \int_{4m_{\pi^+}}^{m_{\omega} - m_{\pi^0}} dm \\ &\quad \times \frac{m^2 \Gamma_{\omega \rightarrow \rho^0 \pi^0}(m) \Gamma_{\rho \rightarrow 2\pi^+ 2\pi^-}(m)}{|D_{\rho}(m^2)|^2} \\ &= 1.1 \times 10^{-9} \end{aligned} \quad (4.9)$$

where

$$\begin{aligned} \Gamma_{\omega \rightarrow \rho^0 \pi^0}(m) &= g_{\omega\rho\pi}^2 q^3(m_{\omega}, m, m_{\pi^0}) / 12\pi, \\ g_{\omega\rho\pi} &= \frac{N_c g^2}{8\pi^2 f_{\pi}} = 14.3 \text{ GeV}^{-1}, \end{aligned}$$

and the numerical data for the  $\rho \rightarrow 2\pi^+ 2\pi^-$  decay width obtained in Sec. III are used. Note also the  $a^{-1}$  dependence of the  $\omega \rightarrow 5\pi$  width on the HLS parameter  $a$ . The branching ratio  $B_{\omega \rightarrow \pi^+ \pi^- 3\pi^0}$  is obtained from Eq. (4.9) upon changing the lower integration limit to  $m_{\pi^+} + 3m_{\pi^0}$ , the substitution  $m_{\pi^0} \rightarrow m_{\pi^+}$  in the expression for the momentum  $q$ , and the substitution of the  $\rho^+ \rightarrow \pi^+ 3\pi^0$  decay width numerically calculated in Sec. III, instead of the  $\rho \rightarrow 2\pi^+ 2\pi^-$  one. Note that the former is corrected for the mass difference of charged and neutral pions. Of course, the main correction of this sort comes from the phase space volume of the final  $4\pi$  state. One obtains

$$\begin{aligned} B_{\omega \rightarrow \pi^+ \pi^- 3\pi^0} &= \left| 1 - \frac{D_{\rho}(\overline{m_{4\pi}^2})}{2D_{\rho}(\overline{m_{2\pi}^2})} \right|^2 \left( \frac{5}{2} \right)^2 \frac{2}{\pi \Gamma_{\omega}} \\ &\quad \times \int_{m_{\pi^+} + 3m_{\pi^0}}^{m_{\omega} - m_{\pi^+}} dm \\ &\quad \times \frac{m^2 \Gamma_{\omega \rightarrow \rho^+ \pi^-}(m) \Gamma_{\rho^+ \rightarrow \pi^+ 3\pi^0}(m)}{|D_{\rho}(m^2)|^2} \\ &= 8.5 \times 10^{-10}, \end{aligned} \quad (4.10)$$

where

$$\Gamma_{\omega \rightarrow \rho^+ \pi^-}(m) = g_{\omega\rho\pi}^2 q^3(m_{\omega}, m, m_{\pi^+}) / 12\pi.$$

As is pointed out in Ref. [2], the inclusion of the direct  $\omega \rightarrow \pi^+ \pi^- \pi^0$  vertex reduces the  $3\pi$  decay width of the  $\omega$  by 33%. This implies that one should make the following replacement to take into account the effect of the pointlike diagrams in Fig. 10(b) in the expression for the suppression factor:

$$\begin{aligned}
\left|1 - \frac{D_\rho(\overline{m_{4\pi}^2})}{2D_\rho(\overline{m_{2\pi}^2})}\right|^2 &\rightarrow \left|1 - \frac{D_\rho(\overline{m_{4\pi}^2})}{2} \left[ \frac{1}{D_\rho(\overline{m_{2\pi}^2})} \right. \right. \\
&\quad \left. \left. - \frac{1}{3m_\rho^2} \right]\right|^2 \approx \left|1 - \frac{D_\rho(\overline{m_{4\pi}^2})}{3D_\rho(\overline{m_{2\pi}^2})}\right|^2 \\
&\simeq 0.75,
\end{aligned} \tag{4.11}$$

instead of 0.64, which results in the increase of the above branching ratios by the factor of 1.17.

The numerical value of the  $\omega \rightarrow 5\pi$  decay width changes by the factor of two when varying the energy within  $\pm\Gamma_\omega/2$  around the  $\omega$  mass. In other words, the dependence of this partial width on energy is very strong. This is illustrated by Fig. 11 where the  $\omega \rightarrow 5\pi$  excitation curves in  $e^+e^-$  annihilation,

$$\begin{aligned}
\sigma_{e^+e^- \rightarrow \omega \rightarrow 5\pi}(s) &= 12\pi \left(\frac{m_\omega}{E}\right)^3 \Gamma_{\omega e^+e^-}(m_\omega) \\
&\quad \times \frac{\Gamma_\omega B_{\omega \rightarrow 5\pi}(E)}{[(s - m_\omega^2)^2 + (m_\omega \Gamma_\omega)^2]},
\end{aligned} \tag{4.12}$$

are plotted. Here  $B_{\omega \rightarrow 2\pi+2\pi-\pi^0}(E)$  [ $B_{\omega \rightarrow \pi+\pi-3\pi^0}(E)$ ] is given by Eq. (4.9) [(4.10)], respectively, with the substitution  $m_\omega \rightarrow E$ . The mentioned strong energy dependence of the partial width results in the asymmetric shape of the  $\omega$  resonance and the shift of its peak position by +0.7 MeV. As is seen from Fig. 11, the peak value of the  $5\pi$  state production cross section is about 1.5-2.0 femtobarns. Yet the decays  $\omega \rightarrow 5\pi$  can be observable on  $e^+e^-$  colliders. Indeed, with the luminosity  $L = 10^{33}\text{cm}^{-2}\text{s}^{-1}$  near the  $\omega$  peak, which seems to be feasible, one may expect about 2 events per week for the considered decays to be detected at these colliders.

The angular distributions of the final pions should be deduced from the full amplitudes Eqs. (4.1) and (4.2). However, some qualitative conclusions about the angular distributions can be drawn from the simplified expressions Eqs. (4.3), (4.5), (4.6), (4.7). Since helicity is conserved, only the states of the  $\omega(782)$  with the spin projections  $\lambda = \pm 1$  on the  $e^+e^-$  beam axes are populated. Corresponding expressions for the various combination of the final pions can be found in Appendix.

The strong energy dependence of the five pion partial width of the  $\omega$  implies that the branching ratio at the  $\omega$  mass, Eq. (4.8), evaluated above, is slightly different from that determined by the expression

$$B_{\omega \rightarrow 5\pi}^{\text{aver}}(E_1, E_2) = \frac{2}{\pi} \int_{E_1}^{E_2} dE \frac{E^2 \Gamma_\omega B_{\omega \rightarrow 5\pi}(E)}{(E^2 - m_\omega^2)^2 + (m_\omega \Gamma_\omega)^2}. \tag{4.13}$$

Taking  $E_1 = 772$  MeV and  $E_2 = 792$  MeV, one finds  $B_{\omega \rightarrow 2\pi+2\pi-\pi^0}^{\text{aver}}(E_1, E_2) = 9.0 \times 10^{-10}$  and  $B_{\omega \rightarrow \pi+\pi-3\pi^0}^{\text{aver}}(E_1, E_2) = 6.7 \times 10^{-10}$  to be compared to Eqs. (4.9) and (4.10), respectively. In particular, the quantity  $B_{\omega \rightarrow 2\pi+2\pi-\pi^0}^{\text{aver}}(E_1, E_2)$  is the relevant characteristics of this specific decay mode in photoproduction experiments. The Jefferson Lab "photon factory" [24] could also be suitable for detecting the five pion decays of the  $\omega$ . However, in view of the suppression of the  $\omega$  photoproduction cross section by the factor of 1/9 as compared with the  $\rho$  one, the total number of  $\omega$  mesons will amount to  $7 \times 10^8$  per nucleon. Hence, the increase of



intensity of this machine by the factor of 50 is highly desirable, in order to observe the decay  $\omega \rightarrow 5\pi$  and measure its branching ratio. Evidently, the  $\omega$  photoproduction on heavy nuclei is preferable in view of the dependence of the cross section on atomic weight  $A$  growing as  $A^{0.8-0.95}$  [25].

The conclusions about how the angular distributions in the  $\omega$  photoproduction are related with those in  $e^+e^-$  annihilation, are basically similar to those concerning the  $\rho$  photoproduction discussed in Sec. III C. The expressions for these distributions coincide with the corresponding expressions Eqs. (A7), (A8), (A9), and (A10) obtained for the case of  $e^+e^-$  annihilation. The vector  $\mathbf{n}_0$  in those formulas can be treated as pointed along the photon beam direction.

## V. CONCLUSION

The results presented in this paper show that, in the  $\rho \rightarrow 4\pi$  decay amplitude, the contributions of the higher derivatives specified by the term induced by the anomalous Lagrangian of Wess and Zumino, vanish rapidly when decreasing the invariant mass of the four pion system below 700 MeV. The loop corrections are also expected to behave similarly. The decay  $\omega \rightarrow 5\pi$  is of a special interest, because its kinematics is such that the final pions are essentially nonrelativistic, and the above effects are completely suppressed in its decay amplitude. Hence the approach to the decays of the vector mesons  $\rho$  and  $\omega$  presented in this paper is the zero order approximation to the full amplitude, in a close analogy with the Weinberg amplitude in the classical  $\pi\pi$  scattering. Under the approximation of the present paper, all chiral models of the vector meson interactions with pions [15] are indistinguishable in their predictions concerning the many pion branching ratios. Any difference could manifest upon including the higher derivatives and chiral loops. As the next step in the development of the present study, the inclusion of the  $a_1$  meson contribution at the tree level approximation would be important. This could help in extending the validity of the treatment up to the invariant masses just below 910 MeV. The task looks meaningful, since the loop corrections, whose particular manifestation is the finite width effects uncovered to be unimportant at  $m_{4\pi} < 910$  MeV ( see Sec. III), are still expected to be small at these invariant masses.

In our opinion, the above considerations show that the left shoulder of the  $\rho$  peak is the very perspective place to study the effects of chiral dynamics of the vector meson interactions. The  $e^+e^-$  colliders with the large enough luminosity at energies below the  $\rho$  mass could provide the controlled source of soft pions. The role of higher derivatives, loop corrections, and, possibly, the  $\rho'$ ,  $\rho''$  contributions in the low energy effective Lagrangian for the soft pions, as well as various schemes of incorporation of the vector mesons into the chiral approach, can be successfully tested with such machines. The intense beams of photons from the Jefferson Laboratory "photon factory" are also of great importance in achieving the mentioned theoretical goals. Certainly, the measurements of the branching ratio of the five pion decays of the  $\omega$  at the level of  $B_{\omega \rightarrow 5\pi} \sim 10^{-9}$  constitute the real challenge to experimenters, but by the reasons specified above the effects of chiral dynamics of the vector meson interactions are manifested in the decay  $\omega \rightarrow 5\pi$  in the very clean way.

## ACKNOWLEDGMENTS

We are grateful to G. N. Shestakov and A. M. Zaitsev for discussion. The present work is supported in part by grant No. RFBR-INTAS IR-97-232.

## APPENDIX: ANGULAR DISTRIBUTIONS

Here a number of expressions for the angular distributions of various combinations of the final pions in the decays  $\rho \rightarrow 4\pi$  and  $\omega \rightarrow 5\pi$  are given. In what follows, the one photon  $e^+e^-$  annihilation production mechanism for these states is assumed, where the  $e^+e^-$  beam axes is characterized by the unit vector  $\mathbf{n}_0$  directed along the z axes.

### 1. The angular distributions in the $\rho \rightarrow 4\pi$ decay

Taking  $\theta_i, \phi_i$  to be the polar and azimuthal angles of the pion three momentum  $\mathbf{q}_i$ , where the momentum assignment corresponds to Eq. (2.11), one finds the following.

(i) The  $\rho^0 \rightarrow 2\pi^+2\pi^-$  decay. The probability density of the emission of four charged pions can be found directly from the first Eq. (2.11):

$$\begin{aligned}
 w &\propto (\mathbf{q}_1 + \mathbf{q}_2 - \mathbf{q}_3 - \mathbf{q}_4)^2 - [\mathbf{n}_0(\mathbf{q}_1 + \mathbf{q}_2 - \mathbf{q}_3 - \mathbf{q}_4)]^2 \\
 &= \sum_{i=1}^4 \mathbf{q}_i^2 \sin^2 \theta_i + 2|\mathbf{q}_1|(1 - P_{23} - P_{24})|\mathbf{q}_2| \sin \theta_1 \sin \theta_2 \cos(\phi_1 - \phi_2) \\
 &\quad - 2|\mathbf{q}_2|(1 + P_{34})|\mathbf{q}_3| \sin \theta_2 \sin \theta_3 \cos(\phi_2 - \phi_3) \\
 &\quad + 2|\mathbf{q}_3||\mathbf{q}_4| \sin \theta_3 \sin \theta_4 \cos(\phi_3 - \phi_4).
 \end{aligned} \tag{A1}$$

One may use the relation

$$(\varepsilon, q_1 + q_2 + q_3 + q_4) = 0 \tag{A2}$$

that expresses the transverse character of the  $\rho$  polarization four vector  $\varepsilon$ , to get rid of the momenta of negatively charged pions  $q_3$  and  $q_4$ . Then the probability density of the emission of two  $\pi^+$ 's found from the first Eq. (2.11) is

$$\begin{aligned}
 w &\propto (\mathbf{q}_1 + \mathbf{q}_2)^2 - [\mathbf{n}_0(\mathbf{q}_1 + \mathbf{q}_2)]^2 \\
 &= \mathbf{q}_1^2 \sin^2 \theta_1 + \mathbf{q}_2^2 \sin^2 \theta_2 + 2|\mathbf{q}_1||\mathbf{q}_2| \sin \theta_1 \sin \theta_2 \\
 &\quad \times \cos(\phi_1 - \phi_2).
 \end{aligned} \tag{A3}$$

Allowing for Eq. (A2), the angular distribution for the emission of two  $\pi^-$ 's is obtained from Eq. (A3) upon the replacement  $\mathbf{q}_{1,2} \rightarrow \mathbf{q}_{3,4}$ .

(ii) The  $\rho^0 \rightarrow \pi^+\pi^-2\pi^0$  decay. The probability density of the emission of  $\pi^+\pi^-$  pair found from the second Eq. (2.11) in the form

$$\begin{aligned}
 w &\propto (\mathbf{q}_1 - \mathbf{q}_2)^2 - [\mathbf{n}_0(\mathbf{q}_1 - \mathbf{q}_2)]^2 \\
 &= \mathbf{q}_1^2 \sin^2 \theta_1 + \mathbf{q}_2^2 \sin^2 \theta_2 - 2|\mathbf{q}_1||\mathbf{q}_2| \sin \theta_1 \sin \theta_2 \\
 &\quad \times \cos(\phi_1 - \phi_2).
 \end{aligned} \tag{A4}$$

Getting rid of the momentum  $q_2$  one finds the corresponding expression for the final state  $\pi^+2\pi^0$ :

$$\begin{aligned} w &\propto (2\mathbf{q}_1 - \mathbf{q}_3 - \mathbf{q}_4)^2 - [\mathbf{n}_0(2\mathbf{q}_1 - \mathbf{q}_3 - \mathbf{q}_4)]^2 \\ &= 4\mathbf{q}_1^2 \sin^2 \theta_1 + \mathbf{q}_3^2 \sin^2 \theta_3 + \mathbf{q}_4^2 \sin^2 \theta_4 - (1 + P_{34})4|\mathbf{q}_1||\mathbf{q}_3| \sin \theta_1 \sin \theta_3 \cos(\phi_1 - \phi_3) \\ &\quad + 2|\mathbf{q}_3||\mathbf{q}_4| \sin \theta_3 \sin \theta_4 \cos(\phi_3 - \phi_4), \end{aligned} \quad (\text{A5})$$

where  $P_{ij}$  interchanges the pion momenta  $q_i$  and  $q_j$ . In view of Eq. (A2), the angular distribution for the state  $\pi^-2\pi^0$  is obtained from the above upon the replacement  $\mathbf{q}_1 \rightarrow \mathbf{q}_2$  and changing the signs in front of the terms containing  $(1 + P_{34})$ .

## 2. The angular distributions in the $\omega \rightarrow 5\pi$ decay

In what follows the suitable notation for the vector product of the pion momenta are used:

$$\begin{aligned} [\mathbf{q}_i \times \mathbf{q}_j] &= |\mathbf{q}_i||\mathbf{q}_j| \sin \theta_{ij} \\ &\quad \times (\sin \Theta_{ij} \cos \Phi_{ij}, \sin \Theta_{ij} \sin \Phi_{ij}, \cos \Theta_{ij}). \end{aligned} \quad (\text{A6})$$

In other words,  $\theta_{ij}$  is the angle between the pion momenta  $\mathbf{q}_i$  and  $\mathbf{q}_j$ ,  $\Theta_{ij}$ ,  $\Phi_{ij}$  being the polar and azimuthal angles of the normal to the plane spanned by the momenta  $\mathbf{q}_i$  and  $\mathbf{q}_j$ . Choosing  $\mathbf{n}_0$  to be the unit vector along z axes, the probability density of the emission of two  $\pi^+$ 's with the momenta  $\mathbf{q}_1$ ,  $\mathbf{q}_2$ , and  $\pi^0$  with the momentum  $\mathbf{q}_4$  is represented as

$$\begin{aligned} w &\propto [\mathbf{q}_4 \times (\mathbf{q}_1 + \mathbf{q}_2)]^2 - (\mathbf{n}_0 \cdot [\mathbf{q}_4 \times (\mathbf{q}_1 + \mathbf{q}_2)])^2 \\ &= \mathbf{q}_4^2 \left[ \mathbf{q}_1^2 \sin^2 \theta_{41} \sin^2 \Theta_{41} + \mathbf{q}_2^2 \sin^2 \theta_{42} \sin^2 \Theta_{42} \right. \\ &\quad \left. + 2|\mathbf{q}_1||\mathbf{q}_2| \sin \Theta_{41} \sin \Theta_{42} \sin \theta_{41} \sin \theta_{42} \right. \\ &\quad \left. \times \cos(\Phi_{41} - \Phi_{42}) \right] \end{aligned} \quad (\text{A7})$$

in the case of the final state  $2\pi^+2\pi^-\pi^0$ . Here the momentum assignment is the same as in Eq. (4.1). The angular distribution of two  $\pi^-$ 's with the momenta  $\mathbf{q}_3$ ,  $\mathbf{q}_5$ , and  $\pi^0$  is obtained from Eq. (A7) upon the replacement  $\mathbf{q}_{1,2} \rightarrow \mathbf{q}_{3,5}$ , because the identity

$$\varepsilon_{\mu\nu\lambda\sigma} q_\mu \epsilon_\nu (q_1 + q_2)_\lambda q_{4\sigma} = -\varepsilon_{\mu\nu\lambda\sigma} q_\mu \epsilon_\nu (q_3 + q_5)_\lambda q_{4\sigma}$$

is valid. Since another identity

$$\varepsilon_{\mu\nu\lambda\sigma} q_\mu \epsilon_\nu (q_1 + q_2)_\lambda q_{4\sigma} = -\varepsilon_{\mu\nu\lambda\sigma} q_\mu \epsilon_\nu (q_1 + q_2)_\lambda (q_3 + q_5)_\sigma$$

is valid, one can write the angular distribution that includes four charged pions:

$$\begin{aligned} w &\propto [(\mathbf{q}_1 + \mathbf{q}_2) \times (\mathbf{q}_3 + \mathbf{q}_5)]^2 - (\mathbf{n}_0 \cdot [(\mathbf{q}_1 + \mathbf{q}_2) \times (\mathbf{q}_3 + \mathbf{q}_5)])^2 \\ &= (1 + P_{12})(1 + P_{35})\mathbf{q}_1^2 \mathbf{q}_3^2 \sin^2 \theta_{13} \sin^2 \Theta_{13} \\ &\quad + 2|\mathbf{q}_1||\mathbf{q}_2|(1 + P_{35})\mathbf{q}_3^2 \sin \theta_{13} \sin \theta_{23} \sin \Theta_{13} \sin \Theta_{23} \cos(\Phi_{13} - \Phi_{23}) \\ &\quad + 2|\mathbf{q}_3||\mathbf{q}_5|(1 + P_{12})\mathbf{q}_1^2 \sin \theta_{13} \sin \theta_{15} \sin \Theta_{13} \sin \Theta_{15} \cos(\Phi_{13} - \Phi_{15}) \\ &\quad + 2|\mathbf{q}_1||\mathbf{q}_2||\mathbf{q}_3||\mathbf{q}_5|(1 + P_{35}) \sin \theta_{13} \sin \theta_{25} \sin \Theta_{13} \sin \Theta_{25} \cos(\Phi_{13} - \Phi_{25}). \end{aligned} \quad (\text{A8})$$

Here  $P_{ij}$  interchanges the indices  $i$  and  $j$ . In the case of the final state  $\pi^+\pi^-3\pi^0$  the corresponding probability density can be obtained from Eqs. (4.6) and (4.7) and looks as

$$\begin{aligned} w &\propto [\mathbf{q}_1 \times \mathbf{q}_2]^2 - (\mathbf{n}_0 \cdot [\mathbf{q}_1 \times \mathbf{q}_2])^2 \\ &= \mathbf{q}_1^2 \mathbf{q}_2^2 \sin^2 \theta_{21} \sin^2 \Theta_{21}. \end{aligned} \quad (\text{A9})$$

Here the momentum assignment is the same as in Eq. (4.2). The corresponding angular distribution of one charged, say  $\pi^+$ , and three neutral pions can be obtained from Eqs. (4.6) and (4.7) upon using the identity

$$\varepsilon_{\mu\nu\lambda\sigma} q_\mu \varepsilon_\nu q_{1\lambda} q_{2\sigma} = -\varepsilon_{\mu\nu\lambda\sigma} q_\mu \varepsilon_\nu q_{1\lambda} (q_3 + q_4 + q_5)_\sigma$$

and looks as

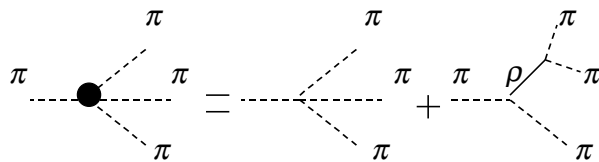
$$\begin{aligned} w &\propto \left[ \mathbf{q}_1 \times \sum_i \mathbf{q}_i \right]^2 - \left( \mathbf{n}_0 \cdot \left[ \mathbf{q}_1 \times \sum_i \mathbf{q}_i \right] \right)^2 \\ &= \mathbf{q}_1^2 \left[ \sum_i \mathbf{q}_i^2 \sin^2 \theta_{i1} \sin^2 \Theta_{i1} \right. \\ &\quad \left. + 2 \sum_{i \neq j} |\mathbf{q}_i| |\mathbf{q}_j| \sin \theta_{i1} \sin \theta_{j1} \sin \Theta_{i1} \sin \Theta_{j1} \right. \\ &\quad \left. \times \cos(\Phi_{i1} - \Phi_{j1}) \right]. \end{aligned} \quad (\text{A10})$$

Here indices  $i, j$  run over 3,4,5.

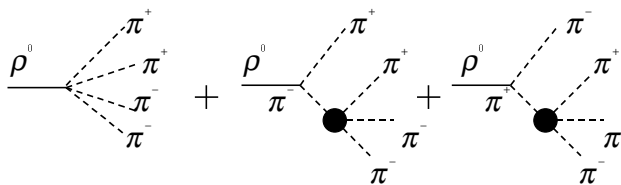
## REFERENCES

- [1] S. Weinberg, *Physica* **96A**, 327 (1979).
- [2] M. Bando, T. Kugo, S. Uehar *et al.*, *Phys. Rev. Lett.* **54**, 1215 (1985); M. Bando, T. Kugo, and K. Yamawaki, *Nucl. Phys.* **B259**, 493 (1985); *Progr. Theor. Phys.* **73**, 1541 (1985); *Phys. Rep.* **164**, 217 (1988).
- [3] N. N. Achasov and A. A. Kozhevnikov, *Phys. Rev.* **D61**, 077904 (2000).
- [4] N. N. Achasov and A. A. Kozhevnikov, *Phys. Lett.* **B480**, 257 (2000).
- [5] A. N. Skrinsky, in: *Proceedings of the "Workshop on Physics and Detectors for DAΦNE'95"* (Frascati Physics Series vol. IV) p. 3; G. Vignola, *ibid.* p. 19.
- [6] A. R. Dzierba, in: *Proceedings from Jefferson Lab/NCSU Workshop on Hybrids and Photoproduction Physics*, (North Carolina State University, Nov. 13-15, 1997) p. 661.
- [7] L. Bányai and V. Rittenberg, *Phys. Rev.* **184**, 1903 (1969).
- [8] A. Bramon, A. Grau, and G. Pancheri, *Phys. Lett.* **B317**, 190 (1993).
- [9] S. I. Eidelman, Z. K. Silagadze, and E. A. Kuraev, *Phys. Lett.* **B346**, 186 (1995).
- [10] R. S. Plant and M. C. Birse, *Phys. Lett.* **B365**, 292 (1996).
- [11] S. L. Adler, *Phys. Rev.* **137**, B1022(1965); *ibid.* **139**, B1638 (1965).
- [12] S. Weinberg, *Phys. Rev.* **166**, 1568 (1968).
- [13] K. Kawarabayashi and M. Suzuki, *Phys. Rev. Lett.* **16**, 255 (1966); Riazuddin and Fayyazuddin, *Phys. Rev.* **147**, 1071 (1966).
- [14] J. Wess and B. B. Zumino, *Phys. Lett.* **37B**, 95 (1971).
- [15] The problem of inclusion of the vector, axial mesons, photons, Z, and W bosons to the framework of chiral theories has demanded considerable efforts. See J. Schwinger, *Phys. Lett.* **24B**, 473 (1967); J. Wess and B. B. Zumino, *Phys. Rev.* **163**, 1727 (1967); S. Gasiorowicz and D. A. Geffen, *Rev. Mod. Phys.* **41**, 531 (1969); O. Kaymakcalan, S. Rajeev and J. Schechter, *Phys. Rev.* **D30**, 594 (1984); U. -G. Meissner, *Phys. Rep.* **161**, 213 (1988), and is solved in an elegant way in the approach based on hidden local symmetry [2]. The interplay between different chiral models with the vector mesons is displayed in the paper M. C. Birse, *Z. Phys.* **A355**, 231 (1996).
- [16] Taking the higher derivatives into account demands also taking into account the chiral loops, the task which is not yet fulfilled for vector mesons.
- [17] R. Kumar, *Phys. Rev.* **185**, 1865 (1969).
- [18] T. W. Sag and G. Szekeres, *Math. Comput.* **18**, 245 (1964).
- [19] C. Caso *et al.*, *Eur. Phys. J.* **C3**, 1 (1998).
- [20] E. Byckling and K. Kajantie, *Particle Kinematics* (John Wiley and Sons, London-New York-Sydney-Toronto, 1973).
- [21] R. R. Akhmetshin *et al.*, *Phys. Lett.* **B475**, 190 (2000).
- [22] Y. S. Tsai, *Phys. Rev.* **D4**, 2821 (1971).
- [23] F. J. Gilman and D. H. Miller, *Phys. Rev.* **D17**, 1846 (1978); F. J. Gilman and S. H. Rhye, *ibid.* **31**, 1066 (1985).
- [24] A. R. Dzierba, in: *Proceedings from Jefferson Lab/NCSU. Workshop on Hybrids and Photoproduction Physics*, (North Carolina State University, November 13-15, 1997) p. 661.
- [25] D. W. G. S. Leith, in: *Hadronic Interactions of Electrons and Photons*, (Academic Press, London and New York, 1971) p.195.
- [26] T. H. Bauer *et al.*, *Rev. Mod. Phys.* **50**, 261 (1978).

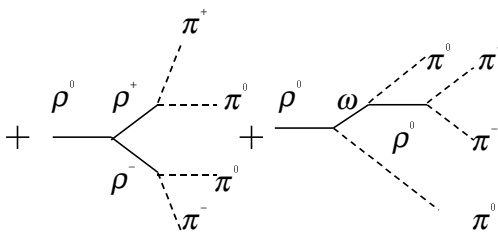
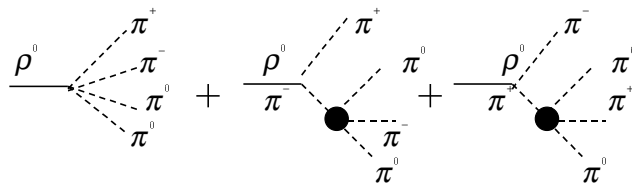
FIGURES



(a)



(b)



(c)

FIG. 1. (a) The diagrams describing the  $\pi \rightarrow 3\pi$  transition amplitude. The symmetrization over momenta of identical pions is understood when necessary. The diagrams describing the amplitudes of the decays (b)  $\rho^0 \rightarrow \pi^+\pi^-\pi^+\pi^-$  and (c)  $\rho^0 \rightarrow \pi^+\pi^-\pi^0\pi^0$ . The shaded circles in the  $\pi \rightarrow 3\pi$  vertices in the diagrams (b) and (c) refer to the sum of diagrams shown in (a). The symmetrization over momenta of identical pions emitted from different vertices is implied. The diagrams for the decays  $\rho^+ \rightarrow \pi^+\pi^0\pi^0\pi^0$  and  $\rho^+ \rightarrow \pi^+\pi^+\pi^-\pi^0$  are analogous to those of (b) and (c), respectively.

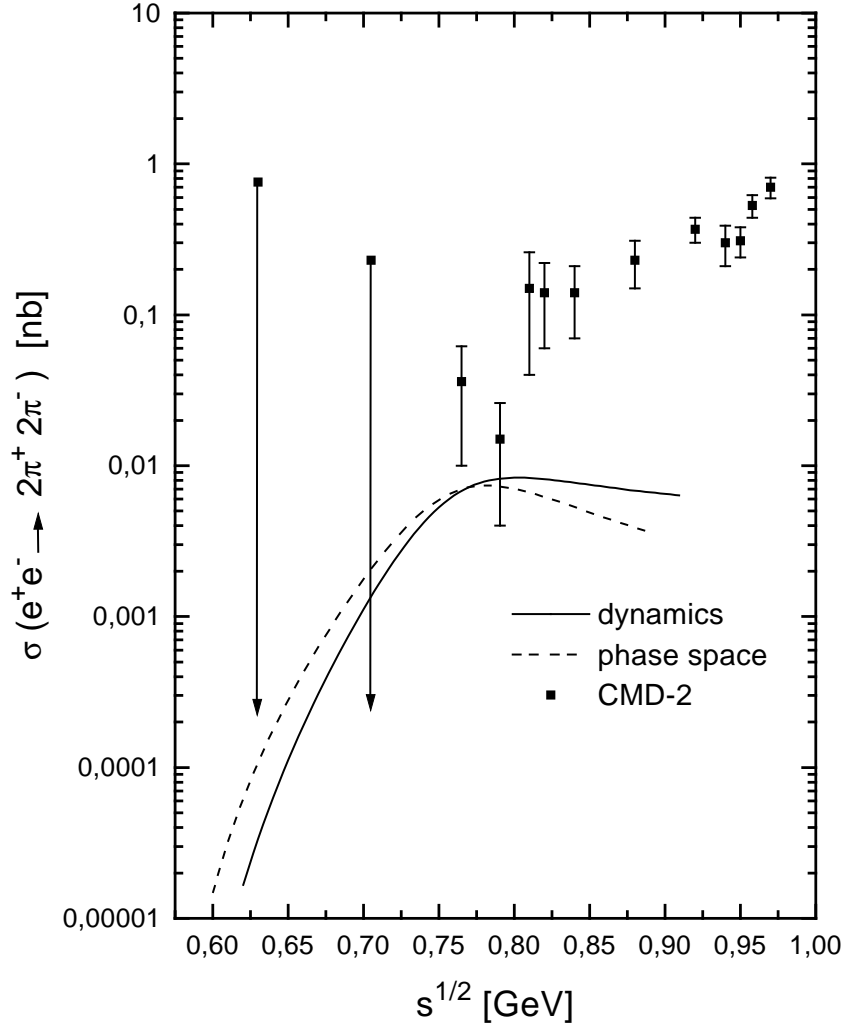


FIG. 2. The energy dependence of the  $e^+e^- \rightarrow \rho^0 \rightarrow \pi^+\pi^-\pi^+\pi^-$  reaction cross section in the model based on the chiral Lagrangian due to Weinberg. Experimental points are from Ref. [21].

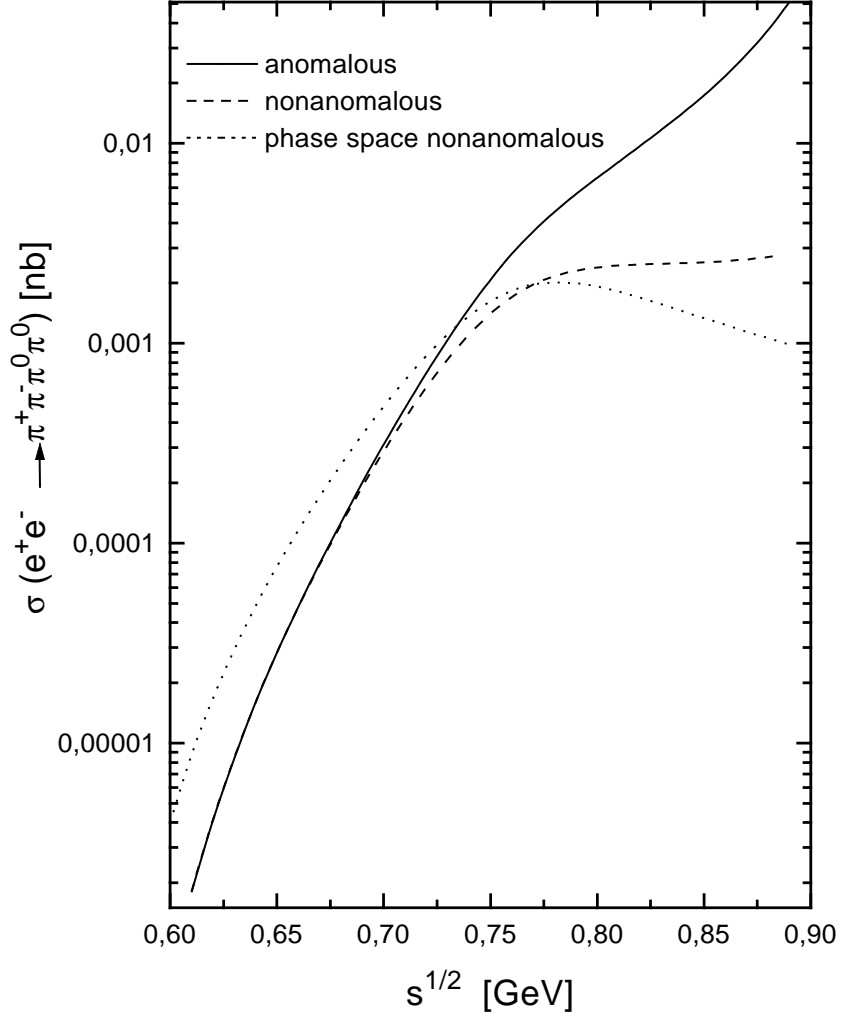


FIG. 3. The energy dependence of the  $e^+e^- \rightarrow \rho^0 \rightarrow \pi^+\pi^-\pi^0\pi^0$  reaction cross section in the model based on the chiral Lagrangian due to Weinberg, added with the terms induced by the anomalous Lagrangian of Wess and Zumino.



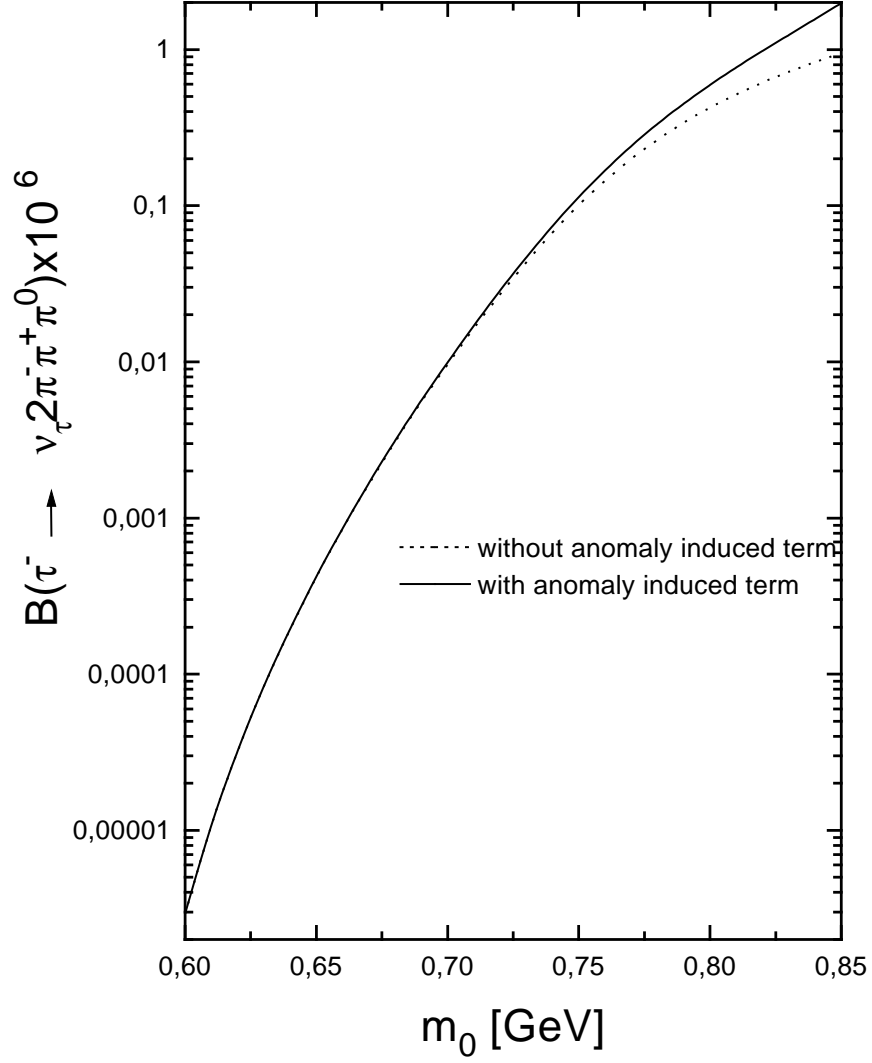


FIG. 4. The dependence of the branching ratio of the decay  $\tau^- \rightarrow \nu_\tau 2\pi^- \pi^+ \pi^0$  on the invariant mass of the four pion system, see Eq. (3.6).

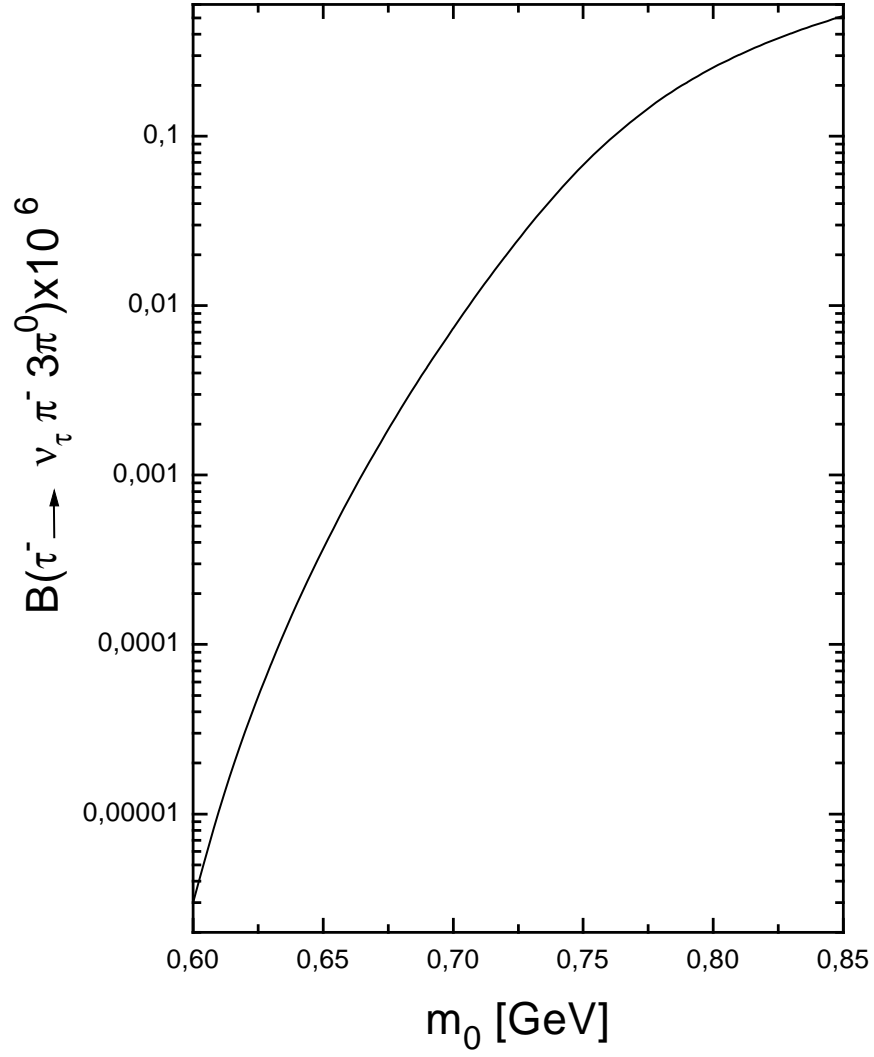


FIG. 5. The same as in Fig. 4, but for the decay  $\tau^- \rightarrow \nu_\tau \pi^- 3\pi^0$ .

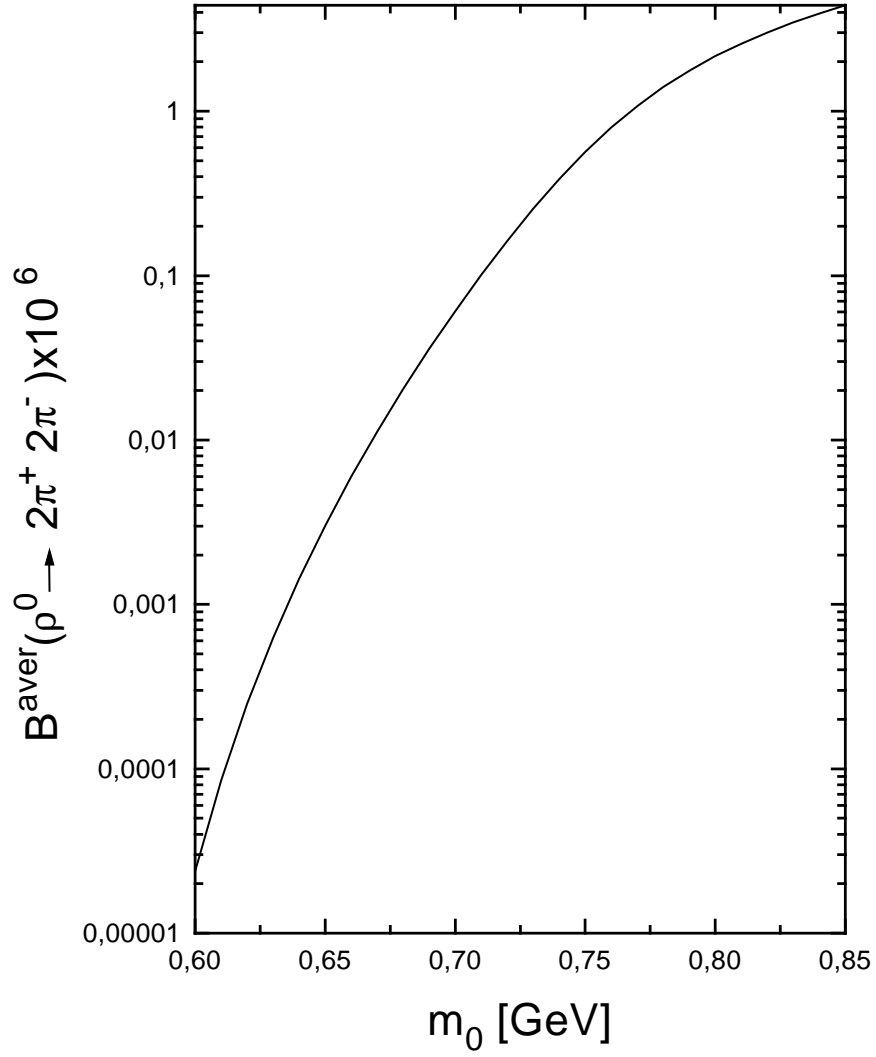


FIG. 6. The dependence of the branching ratio of the decay  $\rho^0 \rightarrow 2\pi^+ 2\pi^-$  averaged over the invariant mass of the four pion system, see Eq. (3.13).

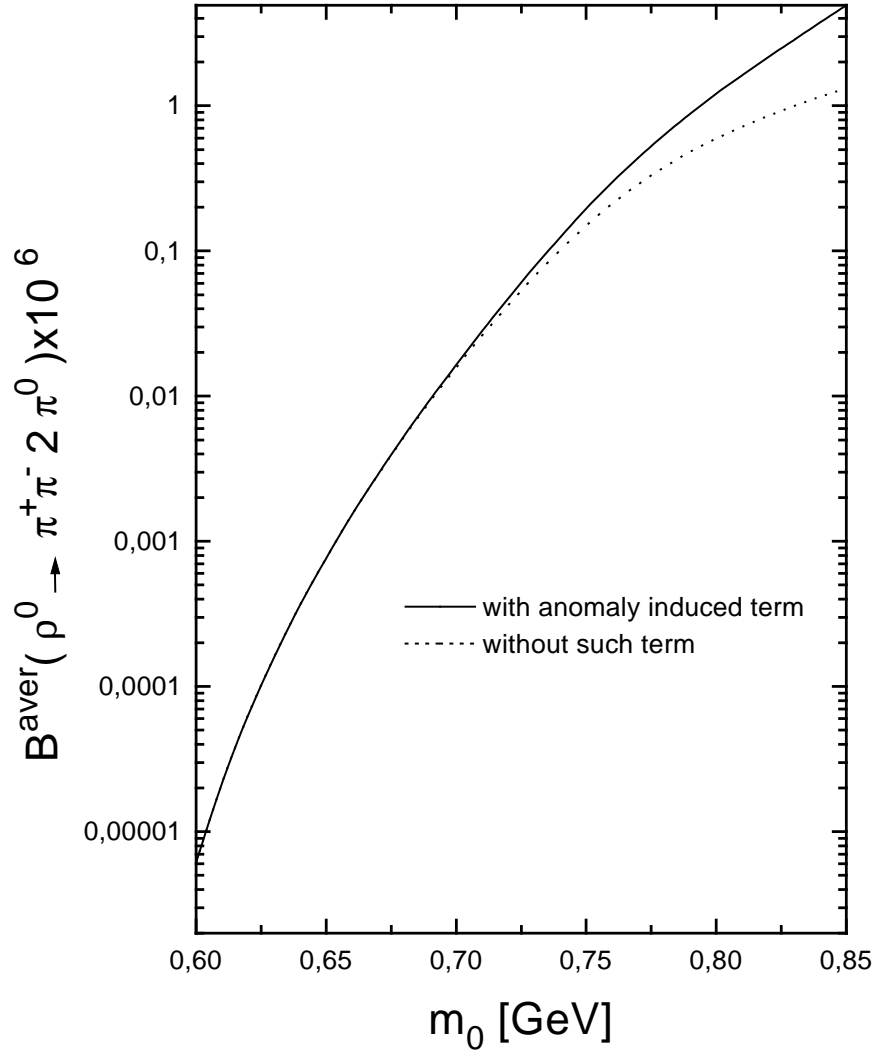


FIG. 7. The same as in Fig. 6 but for the decay  $\rho^0 \rightarrow \pi^+\pi^-2\pi^0$ .

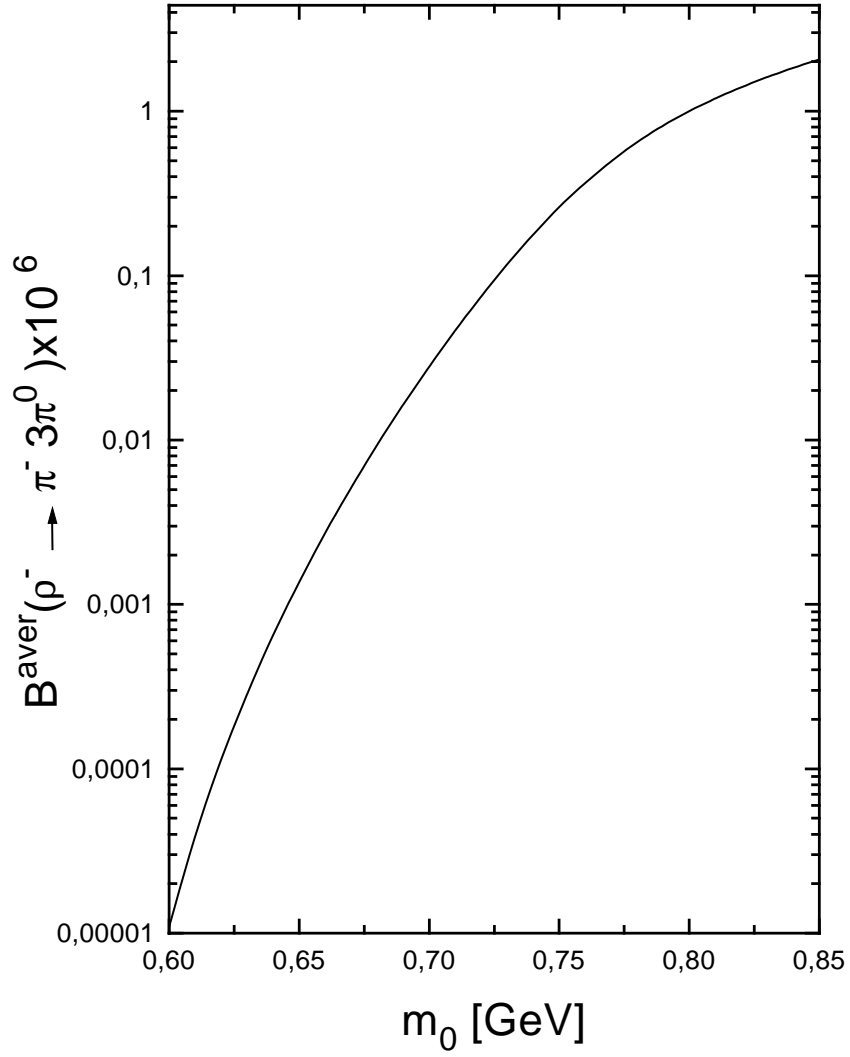


FIG. 8. The same as in Fig. 6 but for the decay  $\rho^- \rightarrow \pi^- 3\pi^0$ .

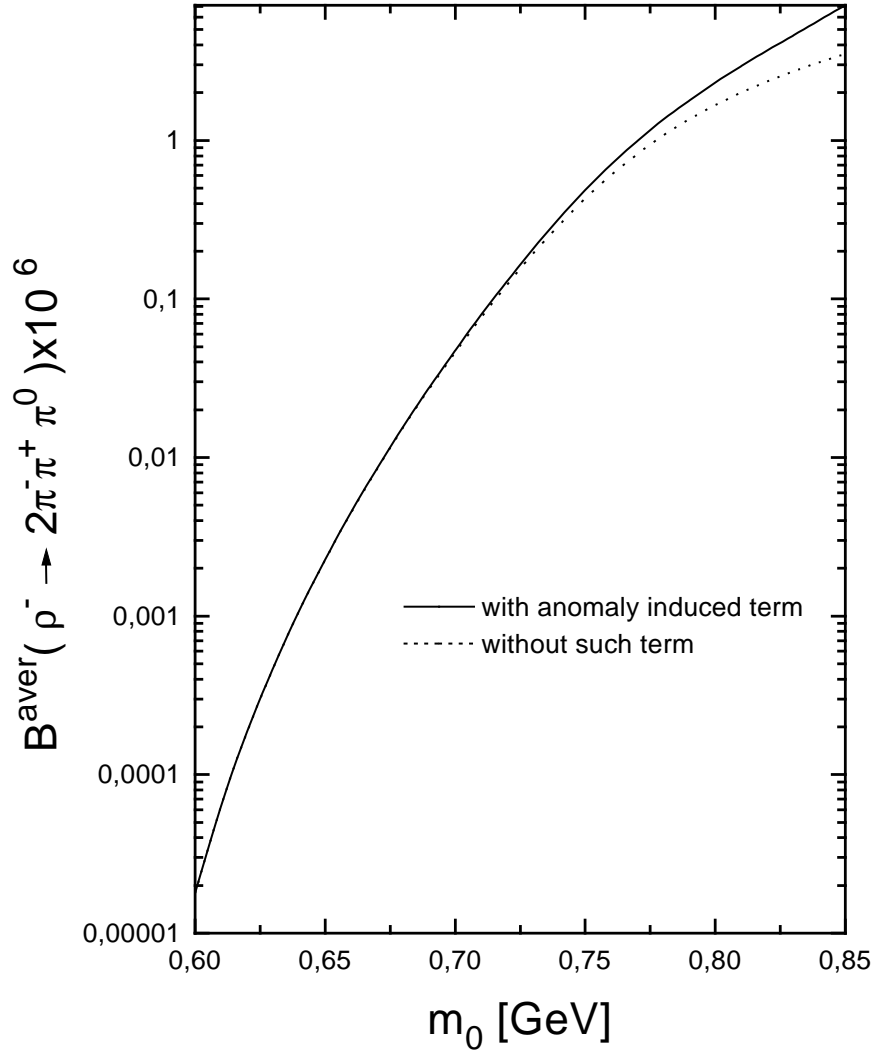


FIG. 9. The same as in Fig. 6 but for the decay  $\rho^- \rightarrow 2\pi^- \pi^+ \pi^0$ .

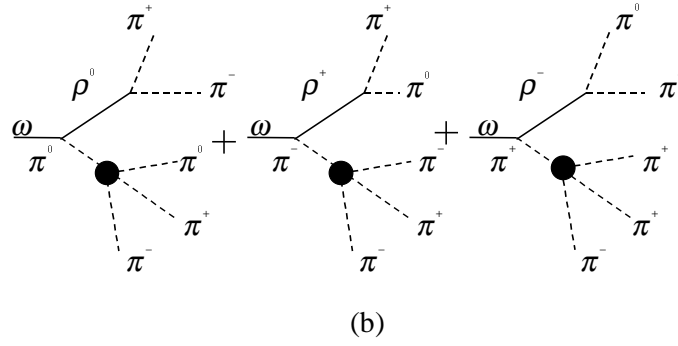
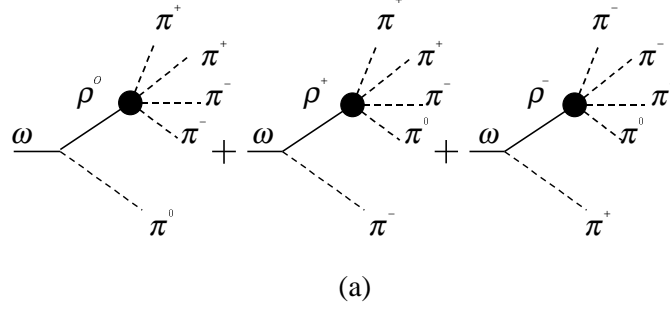


FIG. 10. The diagrams describing the amplitudes of the decays  $\omega \rightarrow \pi^+\pi^-\pi^+\pi^-\pi^0$ . The shaded circles in the set (a) denote the whole set of the  $\rho \rightarrow 4\pi$  diagrams shown in Figs. 1(b), (c). The shaded circles in the  $\pi \rightarrow 3\pi$  vertices in the set (b) refer to the sum of diagrams shown in Fig. 1(a). The symmetrization over momenta of identical pions emitted from different vertices is meant. The diagrams for the decay  $\omega \rightarrow \pi^+\pi^-\pi^0\pi^0\pi^0$  are obtained from those shown upon the evident replacements.

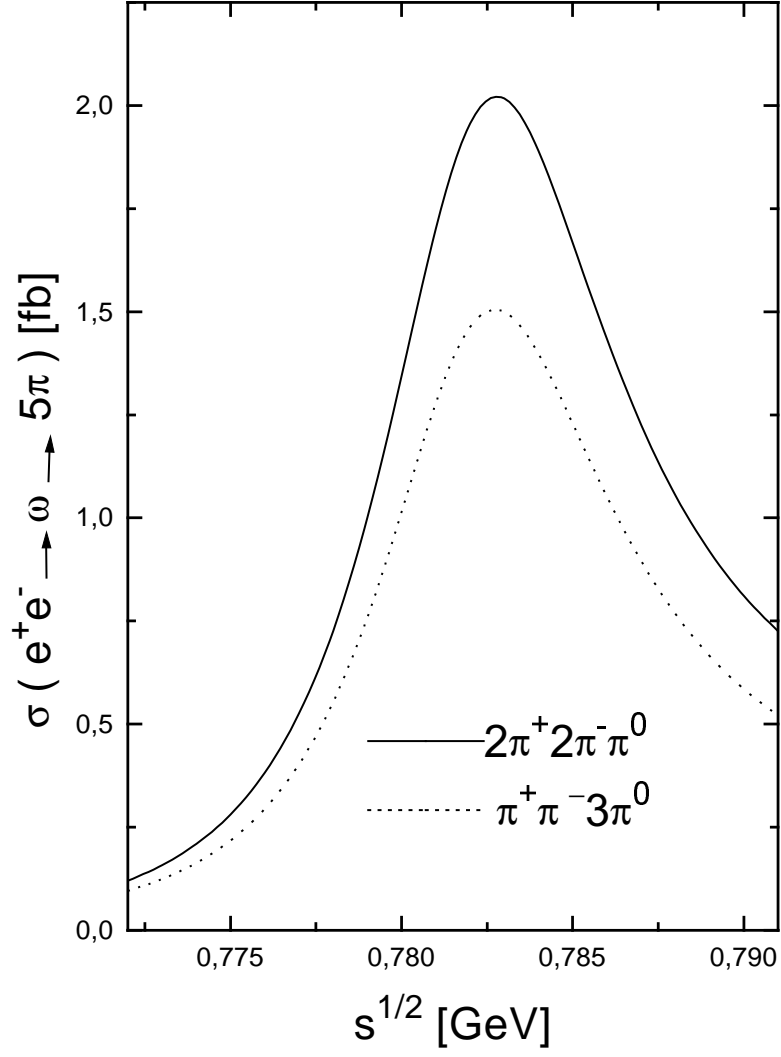


FIG. 11. The  $\omega \rightarrow 5\pi$  excitation curves in  $e^+e^-$  annihilation in the vicinity of the  $\omega$  resonance.